

Micro-CT and Histological Evaluation of a Tissue-Engineered Enthesis in a Rat Model: Comparison to Native Tissue

Carla Konstanze Mayer

Vollständiger Abdruck der von der Fakultät für Medizin der Technischen Universität München zur Erlangung einer Doktorin der Medizin (Dr. med.) genehmigten Dissertation.

Vorsitz: Prof. Dr. Florian Eyer

Prüfer*innen der Dissertation:

1. Prof. Dr. Elizabeth Rosado-Balmayor
2. apl. Prof. Dr. Rainer Burgkart

Die Dissertation wurde am 11.08.2022 bei der Technischen Universität München eingereicht und durch die Fakultät für Medizin am 15.05.2023 angenommen.

DECLARATION

Part of the results gained in this thesis have been previously published in the following publication:

C. J. Peniche Silva, S. A. Müller, N. Quirk, P. S. P. Poh, C. Mayer, A. Motta, C. Migliaresi, M. J. Coenen, C. H. Evans, E. R. Balmayor, M. van Griensven. Enthesis Healing Is Dependent on Scaffold Interphase Morphology—Results from a Rodent Patellar Model. *Cells* **2022**, 11(11), 1752. DOI: 10.3390/cells11111752

I. ABSTRACT

Tendons and ligaments attach to the bone via the osteotendinous junction. This junction is termed enthesis. The enthesis is a unique structure with a gradual transition from soft to hard tissue through four zones. The zonal composition of the enthesis is important for its function as a force transmitter from muscle onto the bone. However, when injured, the healing capacity of the enthesis is low and the zonal structure cannot be restored during regeneration. This posed a challenge to therapy. Current therapeutic strategies are either: conservative, using nonsteroidal anti-inflammatory drugs, cryotherapy, and corticoid injections, or surgical when resecting the necrotic tissue with subsequent suturing of the enthesis onto the bone. Both therapeutic pathways often fail to achieve stable and functionally adequate long-term outcomes. The poor integration of the osteotendinous junction is considered one reason for the unsatisfactory healing. Thus, finding a repair system for the tendon/ligament-to-bone junction is of major clinical interest. One option is to bridge the tissue defects caused by an injury with scaffolds, which overtake the mechanical demands until the regenerative tissue has regained strength and function. Several synthetic and natural origin materials may be suitable as scaffold material. Silk being biodegradable and having mechanical properties similar to tendons and ligaments, makes it attractive as a potential scaffold material for enthesis regeneration.

Previous to this study, biphasic silk-fibroin scaffolds were developed which featured a bone part, a tendon part, and a transition zone. Two types of scaffolds were produced with differences in their transition zone, specifically an abrupt and an interconnected interface were fabricated.

This study aims to evaluate the *in vivo* healing capacity of biphasic silk-fibroin scaffolds in a patella tendon-to-bone enthesis defect model in rats. Five experimental groups with different treatments were included. In four groups tissue defects were created and in one group the patella tendon was cut transversally. In two of the defect groups, the silk-fibroin scaffolds were implanted, in one a collagen sponge was inserted and in one group the defect was bridged with a suture. The samples were harvested for analysis at four

and twelve weeks after implantation. Additionally, native controls were harvested from the contralateral side in four animals. Micro computer-assisted tomography (μ CT) was performed to identify ectopic bone formation in the regenerative area which is a common problem after soft tissue injuries. Moreover, histological evaluations of cell density and alignment, vascularity, and collagen alignment were performed.

After four weeks, no significant differences in the occurrence of ectopic bone formation could be detected between the groups and the contralateral control. After twelve weeks, all experimental groups showed significantly higher levels of ectopic bone formation than the control group. At this time point, the interconnected silk-fibroin scaffold group showed the second-lowest occurrence of ectopic bone formation within the five experimental groups. Cell density was increased in all experimental groups at both time points, parallel cell alignment could be detected in all groups after twelve weeks. Blood vessels were detected in all experimental groups at both time points and collagen alignment was found in both silk-fibroin scaffold groups after twelve weeks. Overall, the group treated with the silk-fibroin scaffold with an interconnected transition showed a lower tendency to develop ectopic bone formation and promising results regarding collagen alignment, cell immigration, and vascularization.

The fact that silk-fibroin scaffolds supported cell immigration is one key finding of this study, as the penetration of the scaffold through cells is of major importance for the initialization of the healing process. These cells can trigger vascularization through growth factors and consequently, necessary nutrients and oxygen are carried to the injury site. Moreover, the regain of an organized extracellular matrix consisting of parallel collagen fibers is essential for the restoration of resistance to mechanical stress.

The findings of this study are encouraging regarding the development of scaffolds for enthesis regeneration. Further biomechanical tests and long-term observations should be considered.

II. ZUSAMMENFASSUNG

Der osteotendinöse Übergang, die sogenannte Enthese, ist die Befestigung von Sehnen oder Bändern am Knochen. Diese Enthese verfügt über eine spezialisierte Struktur, die einen kontinuierlichen Übergang von weichem zu hartem Gewebe gewährleistet und aus vier Zonen besteht. Diese zonenartige Unterteilung ist essenziell für die Funktion als Überträger der Muskelkraft auf den Knochen. Während der Heilung nach Verletzungen der Enthese kommt es häufig zu einer insuffizienten Wiederherstellung der zonalen Struktur, was zu unzufriedenstellender Funktion und schlechten Langzeitergebnissen führt. Dementsprechend besteht ein hohes Interesse darin, eine Lösung mit verbesserten Ergebnissen für die Reparatur von Enthesedefekten zu finden. Eine Möglichkeit ist, die Gewebelücke während der Heilung mit einem Gerüstsystem, einem Scaffold, zu überbrücken. Dieser Scaffold kann, bis das regenerierte Gewebe wieder funktionell ist, die mechanischen Anforderungen der Enthese übernehmen. Es gibt verschiedene synthetische und naturbelassene Materialien, die für die Herstellung solcher Scaffolds in Frage kommen. Seide ist biologisch abbaubar und hat mechanische Eigenschaften, die denen von Sehnen und Bändern gleichen, und kommt deshalb als Scaffoldmaterial in Frage.

Vorliegender Untersuchung ist die Entwicklung von zwei Typen von zweiphasigen Seidenfibroin Scaffolds vorausgegangen. Diese Scaffolds sollen den kontinuierlichen Übergang von weichem zu hartem Gewebe durch unterschiedliche Porosität imitieren und unterscheiden sich in ihrer Übergangszone. Der eine Scaffold hat einen vernetzten und der andere einen abrupten Übergang zwischen den zwei Bereichen.

Die Zielsetzung dieser Arbeit war, die *in vivo* Heilungskapazitäten dieser Scaffolds zu untersuchen. Hierfür wurde ein Rattenmodell mit Patellasehnendefekt entwickelt und fünf experimentelle Gruppen mit unterschiedlichen Behandlungen geschaffen. In vier dieser Gruppen wurden Gewebedefekte geschaffen, in einer ein transversaler Schnitt durch die Patellasehne durchgeführt. In zwei der Defekt-Gruppen wurden Seidenfibroin Scaffolds implantiert, in einer ein Kollagenschwamm eingesetzt und in einer

wurde eine direkte Naht durchgeführt. Vier und zwölf Wochen nach der Implantation erfolgte die Entnahme der Proben. Anschließend wurden Mikrocomputertomographien durchgeführt und es erfolgten histologische Untersuchungen. In den Mikrocomputertomographien wurden heterotope Ossifikationen erkannt, welche ein häufiges Problem bei der Regeneration von Weichgeweben darstellen. In den histologischen Untersuchungen wurden die Zelldichte und Ausrichtung, sowie die Vaskularität und Kollagenanordnung analysiert.

In den vier Wochen nach der Implantation gewonnenen Gewebeproben konnten keine signifikanten Unterschiede im Vorkommen von heterotopen Ossifikationen zwischen den Gruppen und der kontralateralen Kontrolle nachgewiesen werden. Nach zwölf Wochen hatten alle experimentellen Gruppen signifikant höhere Level an heterotopen Ossifikationen als die Kontrollgruppe. Zu diesem Zeitpunkt zeigte die Gruppe, die mit dem Seidenfibroin Scaffold mit vernetztem Übergang behandelt wurde, das zweitniedrigste Vorkommen von heterotopen Ossifikationen. Die Zelldichte und Vaskularität war in allen Gruppen und zu beiden Zeitpunkten erhöht. Ebenso konnten parallele Zellanordnungen in allen experimentellen Gruppen nach zwölf Wochen nachgewiesen werden. Bereiche mit parallel angeordnetem Kollagen zeigten sich nach zwölf Wochen in beiden Gruppen, die mit Scaffolds behandelt wurden. Beachtenswert ist, dass die Scaffoldgruppe mit der vernetzten Übergangszone eine niedrigere Tendenz zur Ausbildung von heterotopen Ossifikationen zeigte und gute Ergebnisse bezüglich der Kollagenanordnung, Zellmigration und Vaskularisierung lieferte. Die Tatsache, dass beide Seidenfibroin Scaffolds die Migration von Zellen in den Scaffold unterstützen, ist vielversprechend, da das Eindringen der Zellen in den Scaffold essenziell für die Initialisierung des Heilungsprozesses ist. Im Scaffold können diese Zellen über Wachstumssignale die Neovaskularisierung auslösen und somit den Transport von Nährstoffen und Sauerstoff zur Regenerationszone gewährleisten. Darüber hinaus ist das Wiedererlangen einer organisierten extrazellulären Matrix mit parallel angeordneten Kollagenfasern wesentlich für die Wiederherstellung von mechanischer Widerstandsfähigkeit.

Die gefundenen Ergebnisse sind zukunftsstrchtig fr die Entwicklung von Scaffolds fr die Regeneration der Enthesis. Weitere biomechanische Tests sowie Langzeitbeobachtungen sind in Betracht zu ziehen.

TABLE OF CONTENTS

I. ABSTRACT	3
II. ZUSAMMENFASSUNG	5
1. ABBREVIATIONS	11
2. INTRODUCTION	12
2.1. BASIC CONCEPTS AND STATE-OF-THE-ART	12
2.1.1. Tendon Anatomy and Function	12
2.1.2. Enthesis Anatomy and Function	13
2.1.3. Ligament, Tendon, and Enthesis Injury	16
2.1.4. Tendon and Enthesis Healing	17
2.2. CLINICAL APPROACHES AND THEIR LIMITATIONS	20
2.3. EXPERIMENTAL APPROACHES AND THEIR LIMITATIONS	22
2.3.1. Tissue Engineering	22
2.3.2. Stem Cells	22
2.3.3. Growth Factors	23
2.3.4. Scaffolds	24
2.4. PREVIOUS EXPERIMENTS AND AIM OF THIS STUDY	26
2.5. EVALUATION METHODS	26
2.6. HYPOTHESIS	27
3. MATERIAL AND METHODS	28
3.1. SCAFFOLD DESCRIPTION	28
3.2. PATELLAR ENTHESIS MODEL	29
3.3. SCAFFOLD IMPLANTATION AND STUDY DESIGN	30
3.4. MICRO-COMPUTED TOMOGRAPHY (μCT)	31
3.5. HISTOLOGY: DECALCIFICATION	32
3.6. HISTOLOGY: PARAFFIN EMBEDDING	33
3.7. HISTOLOGY: SECTIONING	33
3.8. HISTOLOGY: STAINING OF TISSUE SECTIONS	33

3.8.1. Hematoxylin-Eosin Staining	34
3.8.2. Masson-Goldner-Trichrome Staining	34
3.8.3. Picro-Sirius Red Staining	35
3.9. MICROSCOPY	36
3.10. STATISTICAL ANALYSIS OF μCT	36
3.11. HISTOLOGICAL EVALUATION	36
4. RESULTS	37
4.1. EXPERIMENTAL GROUPS	37
4.2. MICRO-CT ANALYSIS.....	38
4.3. HISTOPATHOLOGICAL CHARACTERISTICS	40
4.3.1. Sample Numbers for Histology	40
4.3.2. Cell Density and Alignment to the Longitudinal Axis	41
4.3.3. Vascularity	44
4.3.4. Collagen Alignment	45
5. DISCUSSION	48
5.1. STUDY GROUPS AND TREATMENT	48
5.2. MICRO-CT ANALYSIS	49
5.3. CELL DENSITY AND ALIGNMENT PARALLEL TO THE LONGITUDINAL AXIS	51
5.4. VASCULARITY	53
5.5. COLLAGEN ALIGNMENT	54
5.6. LIMITATIONS AND OUTLOOK	56
5.7. RECAPITULATION AND CONCLUSION	57
6. REFERENCES	59
7. APPENDIX	67
7.1. LIST OF FIGURES	67
7.2. LIST OF TABLES	68
7.3. PERMISSION TO INCLUDE PUBLISHED WORK IN THE DOCTORAL THESIS	68

7.4. MATERIAL LIST.....	70
8. ACKNOWLEDGMENTS	73

1. ABBREVIATIONS

μ	Micro
ACL	Anterior cruciate ligament
ASCs	Adipose-derived stem cells
ADMSCs	Adipose-derived mesenchymal stem cells
BFGF	Basic fibroblast growth factor
Cm	Centimeter
CT	Computer-assisted tomography
EDTA	Ethylenediaminetetraacetic acid
ECM	Extracellular Matrix
EGF	Epidermal growth factor
Fig.	Figure
M.	Musculus
MSC	Mesenchymal stem cell
NaOH	Sodium hydroxide
NSAIDs	Nonsteroidal anti-inflammatory drugs
PBS	Phosphate-buffered saline
PGFG	Platelet-derived growth factor
ROI	Region of interest
TGF-β	Transforming growth factor beta
VEGF	Vascular endothelial growth factor

2. INTRODUCTION

2.1. BASIC CONCEPTS AND STATE-OF-THE-ART

2.1.1. Tendon Anatomy and Function

Tendons are white, brilliant, viscoelastic structures that connect muscles and bones (Franchi, Trire, Quaranta, Orsini, & Ottani, 2007; Snedeker & Foolen, 2017). Their ability to withstand 17 times the body weight is ensured through their anatomy (O'Brien, 2005). They consist of closely packed collagen fibers and tenocytes embedded in extracellular matrix (ECM) (Schneider, Angele, Jarvinen, & Docheva, 2018). Collagen constitutes about 85% of the tendon's dry weight (Kirkendall & Garrett, 1997). The collagen helix is produced in the tenocytes and then extracellularly arranged into microfibrils that form the collagen fibers (James, Kesturu, Balian, & Chhabra, 2008). The collagen fiber is the basic unit of the tendon. Those collagen fibrils are arranged mainly longitudinally but also horizontally and transversely to enable the tendon to transmit forces in different directions. The endotendon, a connective tissue coat, surrounds collagen fiber bunches and forms fiber bundles that merge to the tendon (Kannus, 2000). The endotendon continues as a covering tissue layer around the tendon, the epitendon. The epitendon ensures mobility in the surrounding tissue. It contains blood vessels and nerves and thereby guarantees the supply of nutrients and oxygen to the tendon (Thorpe & Screen, 2016).

Tendon's function is to gather muscular force on the myotendinous junction and transmit it onto the bone at the osteotendinous junction, the enthesis (Wu, Nerlich, & Docheva, 2017). Tendons are specialized anatomical structures that adapt to functional demands. For example, the load at failure and the collagen content of tendons increase through training (Wang, 2006). Anyhow, tendons have a low metabolic rate and comparably low vascularization. In long tendons, such as the Achilles tendon, hypovascular zones of two to six centimeters (cm) occur (Wu et al., 2017). This leads to a lower

regeneration capacity and higher vulnerability in cases of overuse. As mentioned, the Achilles tendon is very poorly vascularized and thereby especially susceptible for degeneration (M. Benjamin, Kaiser, & Milz, 2008). Additionally, the tendon-to-bone junction is sensitive for overuse injuries (Wang, 2006). Figure (Fig.) 1 illustrates the basic microscopic anatomy of a tendon.

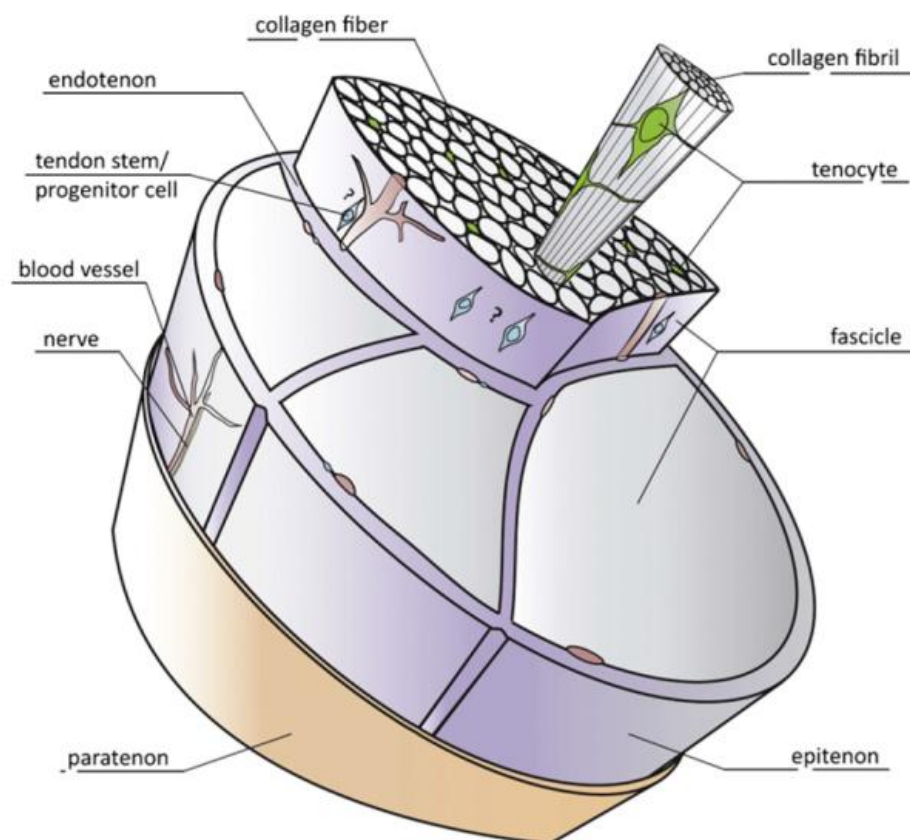


Fig. 1: Tendon structure. Reprinted with permission from Elsevier from (Docheva, Muller, Majewski, & Evans, 2015).

2.1.2. Enthesis Anatomy and Function

The enthesis represents the transition of soft tissue (tendon or ligament) to hard tissue (bone) (Shaw & Benjamin, 2007).

Two different kinds of entheses can be distinguished: the fibrous and the fibrocartilaginous (Michael Benjamin et al., 2003). Characteristically, fibrous entheses attach through short tendons and over large areas at the diaphysis of bones (Tadros, Huang, &

Pathria, 2018). Microscopically, they consist of mineralized collagen fibers that perforate into the adjacent bone (Apostolakos et al., 2014). As the fibrocartilaginous enthesis is the more common type of osteotendinous junction (Thomopoulos, Genin, & Galatz, 2010) and the analyzed tibial insertion of the patella tendon is a fibrocartilaginous enthesis (M. Benjamin et al., 2006), this thesis will be focusing on this kind of insertion and refer to fibrocartilaginous entheses as entheses. Fibrocartilaginous entheses mainly attach on the epi- and apophysis of the bones, e.g., at the rotator cuff, the Anterior cruciate ligament (ACL) or the Achilles tendon (Apostolakos et al., 2014; H. H. Lu & Thomopoulos, 2013). The microscopic structure consists of four zones: a tendinous part, non-mineralized fibrocartilage, mineralized fibrocartilage, and the bone it connects to. The alignment of the collagen builds on towards the tendon/ligament while the mineralization increases towards the bone (Font Tellado et al., 2017). This structural particularity is of major importance for a functional force transmission (Moffat et al., 2008).

The content of unmineralized fibrocartilage is increased in entheses with an acute angle of insertion such as at the femoral ACL enthesis (Beaulieu, Carey, Schlecht, Wojtys, & Ashton-Miller, 2015). As the content of unmineralized fibrocartilage is higher in entheses with lots of change in their insertion angle during movement, the tissue seems to specialize according to the local demands. Moreover, the amount of fibrocartilage in entheses appears to be positively related to the size of the cross-sectional area (Evans, Benjamin, & Pemberton, 1990). The strain on the insertion site decreases from the tendon towards the bone, whereas stiffness and the mineral content increases towards the bone (Moffat et al., 2008).

The blood supply on the osteotendinous junction is assured through the bone, yet it is confined to the insertion area (Carr & Norris, 1989). Fibrocartilages are avascular which leads to minor healing capacity in this area (M. Benjamin et al., 2006).

The enthesis' elementary function is to secure a stable anchoring of the ligament or tendon at the bone end. As a result, all mechanical stress during movement concentrates on a small area at the enthesis which makes it prone to overuse (M. Benjamin et al., 2006). In order to reduce the stress on the insertion site, tendons and ligaments often spread out at their attachment to the skeleton and blend with neighboring structures (M. Benjamin et al., 2004). Another strategy to reduce stress at the enthesis, is to form firmer and more strain-bearing bundles, at locations where several tendons attach. The *pes anserinus*, where musculus (M.) semitendinosus, M. gracilis and M. sartorius insert, is an example of this (Shaw & Benjamin, 2007). The components and the microscopic structure of the enthesis are illustrated in figure 2 and 3.

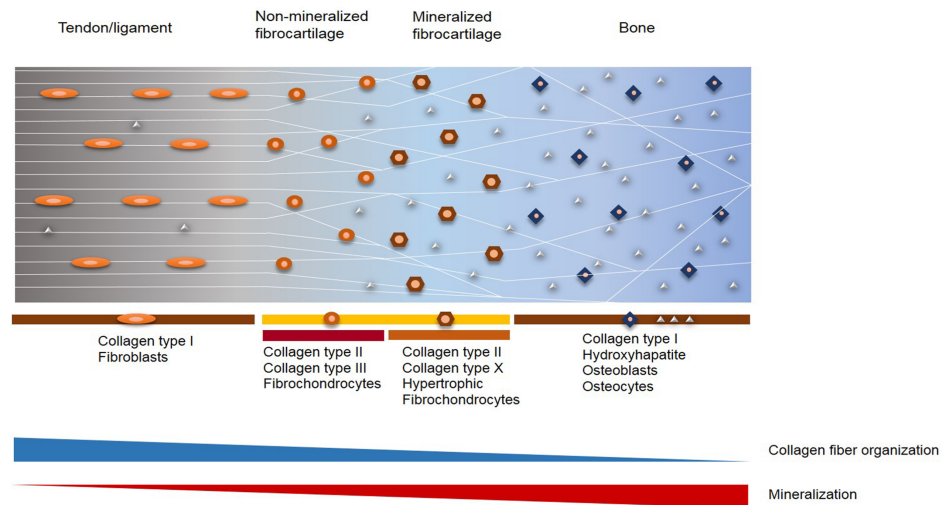


Fig. 2: Structure and composition of fibrocartilaginous enthesis. Reprinted with permission from Elsevier from (Font Tellado, Balmayor, & Van Griensven, 2015).

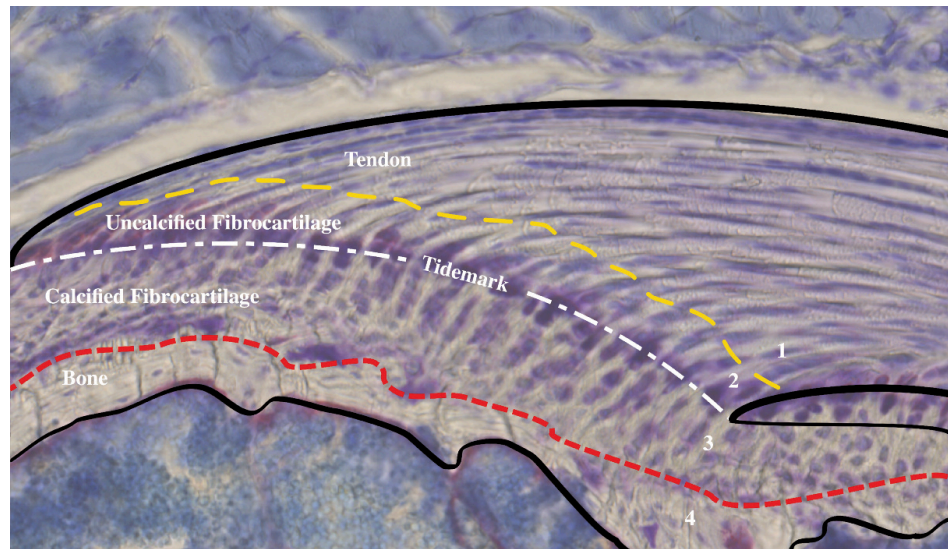


Fig. 3: Illustration of the four zones of the enthesis in a mouse supraspinatus. Staining in toluidine blue. Reprinted with permission from Edra SpA from (Apostolakos et al., 2014).

2.1.3. Ligament, Tendon, and Enthesis Injury

Tendons are able to bear and buffer high forces and thereby protect the muscles from damage. This high mechanical load makes them vulnerable to injuries. It is assumed that more than 50 percent of the 30 million musculoskeletal injuries reported worldwide involve tendons and ligaments (Gaspar, Spanoudes, Holladay, Pandit, & Zeugolis, 2015). Tendons often affected by degeneration are the Achilles tendon, the tendons of the rotator cuff, or the patella tendon (Docheva et al., 2015). In Germany, the annual incidence of Achilles tendon ruptures is 20/100.000 and has a rising tendency (Mueller, 2011). In the United States, more than 250.000 rotator cuff repairs and more than 100.000 ACL reconstructions are performed annually (Butler et al., 2008; Jain et al., 2014). These data show that an understanding of the pathologies, healing, and treatment of tendons, ligaments, and their entheses is of high clinical relevance. Populations in which tendon injuries occur are, on one hand, physically active adults and, on the other hand, moderately active elderly people (Wu et al., 2017). The incidence of tendon injuries is expected to increase, as the number of elderly and at the same time

active people rises (Butler et al., 2008). A distinction is made between acute tendon injuries, happening as a result of sudden overload, and, more commonly, tendon ruptures because of chronic overuse. A persistent strain on the tendon causes microtrauma and the continuation of stress hinders the healing of these lesions (Hyman & Rodeo, 2000; Selvanetti, Cipolla, & Puddu, 1997). This can lead to degeneration, tendinopathies, and ruptures (Walden et al., 2017). Tendinopathies are described as pain and loss of function in tendons (Lipman, Wang, Ting, Soo, & Zheng, 2018). There are extrinsic factors (e.g., sport or physical activity) and intrinsic factors, such as age, sex, diabetes, rheumatoid arthritis, or genetic predisposition, that support the development of tendinopathy (Riley, 2004). In a study by Kannus and Jozsa, degenerative changes were found in 97% of the spontaneously ruptured tendons. For comparison, similar degenerative changes were found in only 33% of the control (Kannus & Jozsa, 1991). Inflammation of the coating structures or degeneration of the load-bearing elements are potential reactions to overuse (Benazzo, Zanon, & Maffulli, 2000). Deterioration of collagen, increase of overall cellularity, and simultaneous necrosis of tenocytes can intensify inflammation and increase the rupture risk (Dean, Franklin, & Carr, 2012; Khan, Cook, Bonar, Harcourt, & Astrom, 1999; Pankaj Sharma & Maffulli, 2005). Typical locations of tendon ruptures are at the myotendinous, osteotendinous junction, or avulsion fractures, rather than mid-tendon ruptures (Taylor, Dalton, Seaber, & Garrett, 1993).

2.1.4. Tendon and Enthesis Healing

Tendon healing is a lengthy process that is still not completely understood. There are three main stages during tendon healing (Hope & Saxby, 2007).

Firstly, the inflammatory stage starts immediately after injury and takes a few days. The tendon rupture causes the tear of blood vessels and thereby the formation of a hematoma (Lin, Cardenas,

& Soslowsky, 2004). Pro-inflammatory cytokines are released, initiating the blood cells (e.g. platelets) and inflammatory cells (e.g., neutrophils and monocytes) (Wu et al., 2017). In the early stage of tendon healing, angiogenesis is initialized by growth factors, for example, vascular endothelial growth factor (VEGF) (Bidder, Towler, Gelberman, & Boyer, 2000; Fenwick, Hazleman, & Riley, 2002). Moreover, basic fibroblast growth factor (bFGF), transforming growth factor beta (TGF- β), epidermal growth factor (EGF), and platelet-derived growth factor (PDGF) are found in cells during tendon repair and presumably take a role in the initialization of neovascularization (Chang et al., 1998; Duffy, Seiler, Gelberman, & Hergueter, 1995; Kuroda, Kurosaka, Yoshiya, & Mizuno, 2000). Macrophages digest necrotic material from the injury site. Furthermore, the proliferation of tenocytes is initiated, and the synthesis of collagen type III is enhanced (Hoffmann & Gross, 2006; Voleti, Buckley, & Soslowsky, 2012).

Secondly, the proliferation stage takes a few weeks. High cellularity and water absorption are characteristic of this stage. The production of extracellular matrix components, for example, collagen type III and proteoglycans starts and their disposition happens randomly (Wu et al., 2017). Macrophages induce cell recruitment through growth factors. Migration of fibroblasts from the epitendon and synovial sheath to the injury site takes place. The replacement of collagen type III by the stronger collagen type I begins and will gradually continue over the healing process (Schneider et al., 2018).

Thirdly, the remodeling stage takes place. It is divided into the consolidation stage which lasts up to ten weeks and then followed by the maturation stage which can take up to two years. The duration of these healing processes is contingent on factors like the patient's age and health conditions (Docheva et al., 2015). The consolidation stage is defined by the change of highly cellular tissue to more fibrous tissue. Tenocytes and collagen fibers align themselves in the direction of the strain and thereby regain strength

and rigidity. This effect is intensified by the ongoing production of type I collagen (Pankaj Sharma & Maffulli, 2005). As tendon fibroblasts develop into contracting myofibroblasts, the large granulation tissue shrinks into scar tissue. The change of fibrous tissue into scar tissue is characterizing the final maturation stage and involves the decrease of the tenocyte's metabolism and tendon vascularity (Schneider et al., 2018).

The following figure visualizes the three stages and the basic processes of tendon healing.

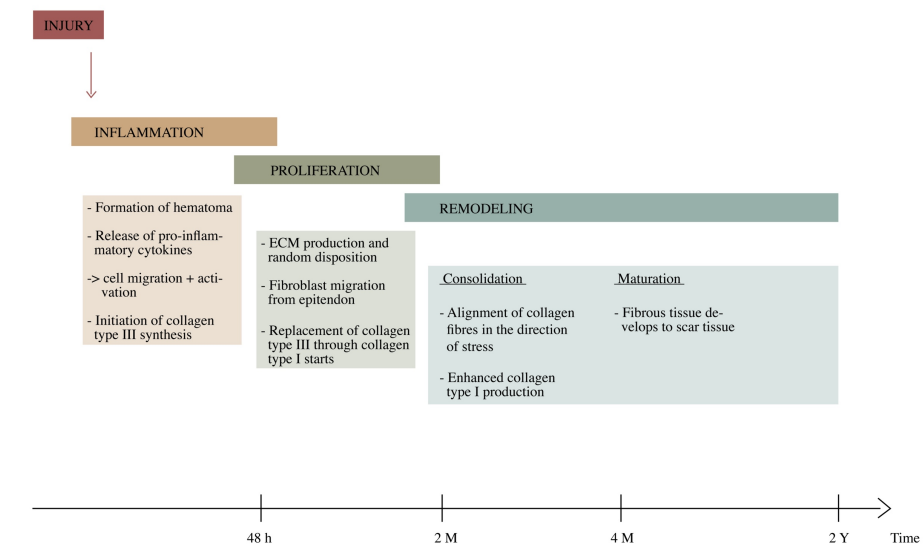


Fig. 4: Stages of tendon repair. In the timeline: h = hours, M = months, and Y = years.

Overall, tendon healing involves extrinsic as well as intrinsic healing. Extrinsic healing means that fibroblasts and inflammatory cells migrate from the periphery to the injury site. This happens mainly during the early stages. Intrinsic healing is seen as the migration of cells from the endotendon to the injury site where proliferation starts and the production and organization of ECM is initialized (James et al., 2008).

The high mechanical demand on the tendon induces thickening and thereby stiffness. Making the tendon vulnerable to re-rupture (Schneider et al., 2018). Although tendon healing has been

investigated and knowledge about cells and molecular factors has been gained, there is still a lack of sufficient therapies for tendon injury (Wu et al., 2017).

The knowledge about the role of the tendon-to-bone junction after an injury is limited. It was seen that a strong healing response occurs when a ruptured tendon is securely sutured onto the bone, but this creates a sharp junction between unorganized collagen and bone. A regain of the zonal structure with a gradient of mineralization could not be detected. (H. H. Lu & Thomopoulos, 2013). This unstructured transition zone cannot keep up with the mechanical properties of a native enthesis. (Burkhart, Johnson, Wirth, & Athanasiou, 1997; Smietana, Moncada-Larrotiz, Arruda, Bedi, & Larkin, 2017). Even though structural characteristics in surgically sutured supraspinatus enthesis injuries in a rat model resembled the native enthesis to three-thirds after eight weeks, mechanical properties remained inferior (Thomopoulos, Williams, & Soslowky, 2003). Furthermore, a loss in bone mineral density has been reported in rotator cuff tears in a rat model. It was shown that the bone loss hinders the healing of the enthesis and might lead to a deterioration of the resilience (Galatz et al., 2005).

2.2. CLINICAL APPROACHES AND THEIR LIMITATIONS

Generally, injuries of the tendon and enthesis can either be treated conservatively or by surgery. For minor injuries, conservative therapy is eligible. This includes rest, nonsteroidal anti-inflammatory drugs (NSAIDs), cryotherapy, and corticosteroid injections (Calejo, Costa-Almeida, Reis, & Gomes, 2019; Lim, Liao, Ng, Chowdhury, & Law, 2019). Whatsoever, conservative therapy has its limitations. Up to 29% of the patients initially treated conservatively, must eventually get surgery due to unsatisfactory results (Zafar, Mahmood, & Maffulli, 2009).

For tendon lesions wider than 5mm, surgery is the only chance of restoring tissue function for active patients. During surgery necrotic parts are resected and either an end-to-end tendon suture or a tight

suture onto the bone is performed (Rawson, Cartmell, & Wong, 2013; Smietana et al., 2017). As stated in the last paragraph, tendon tissue and the tendon-to-bone interface both feature limited healing capacity. The regenerated tissue will not gain the same strength as the native one. This leads to re-rupture rates up to 94% after arthroscopic repair of massive rotator cuff tears (Galatz, Ball, Teefey, Middleton, & Yamaguchi, 2004). Additionally, long-term complications such as post-operative osteoarthritis and chronic pain can develop (Walden et al., 2017). In some cases, with heavily damaged native tissue, a direct suture is not eligible as a therapeutic option. Then, autografts, allografts, or xenografts are used (Lomas et al., 2015). Autografts, commonly harvested from the hamstrings, the patellar, or the quadriceps tendon, are the gold-standard (Shelton & Fagan, 2011). Although autografts create a similar structure to the native tissue, remodeling and healing lead to minor tissue quality and inferior mechanical properties. Re-rupture rates vary between 35 and 95% (Snedeker & Foolen, 2017). Moreover, donor-site morbidity, resulting in pain, muscular weakness, and an increased risk of injury at the donor site are disadvantages of autografts (Shelton & Fagan, 2011). In allografts, immune reaction, allergy, and infection risks are possible causes of therapy failure (Kaeding et al., 2011; Lomas et al., 2015). A common problem after tendon or enthesis injuries is trauma acquired ectopic bone formation (Xu, Hu, Zhou, & Yang, 2018). Two different forms of acquired heterotopic ossification can be distinguished. There is a non-cell-mediated and a cell-mediated heterotopic ossification. The first is seen as the direct accumulation of calcium salts. The second form is initialized by the activation of osteoblasts by a process in which unmineralized bone matrix develops into mineralized bone (Zhang, Zhou, Wang, & Tan, 2020). Triggers such as inflammation, injury, and hypoxia lead to the differentiation of progenitor cells into bone and cartilage (Davis et al., 2011; Kokubu, Inaki, Hoshi, & Hikita, 2020; Zhang et al., 2020). The occurrence of heterotopic bone formation leads to extended healing processes and higher morbidity (Davis et al., 2011).

In the prevention of heterotopic ossification, bisphosphonates, NSAID, and radiation are commonly used. Nevertheless, none of the above named is able to impede heterotopic ossification sufficiently (Board, Karva, Board, Gambhir, & Porter, 2007; Cai, Wang, Luo, She, & Zhang, 2019; Zhang et al., 2020). Once heterotopic ossification has occurred, physiotherapy is an option to slow down the development of stiffness. Another method is the surgical excision of the ectopic bone (Board et al., 2007). Though the risk to induce the formation of ectopic bone formation by the tissue trauma is undeniable (Xu et al., 2018).

2.3. EXPERIMENTAL APPROACHES AND THEIR LIMITATIONS

2.3.1. Tissue Engineering

For the treatment of difficult injuries, tissue engineering has developed as an uprising field of science (Butler et al., 2008). Tissue engineering is an interdisciplinary domain that unites science and engineering in order to generate substitutes that are able to regain tissue function (Langer & Vacanti, 1993). It is a field that intends to support the body's repair capacity (Walden et al., 2017). Tissue engineering strives to improve tissue regeneration using three central pillars: stem cells, supportive biological factors, and scaffolds (Ali Moshiri & Oryan, 2012).

2.3.2. Stem Cells

Cell-based therapies are one central pillar of tissue engineering (A. Moshiri, Oryan, & Meimandi-Parizi, 2013). For example, mesenchymal stem cells (MSCs) are cells that are able to differentiate into cell types, such as osteoblasts, chondrocytes, and fibroblasts. Direct injection or delivery on a scaffold are options to apply MSCs to the tendon healing site (Awad et al., 1999; Young et al., 1998). As MSCs can differentiate into various cell types present at the osteotendinous junction, they should be taken into consideration for tissue-engineered enthesis regeneration. It may be speculated that *in vivo* the neighboring tissue should be able to signal MSC differentiation in the direction of bone or tendon (Font

Tellado et al., 2015). The promotion of a controlled cellular differentiation depending on the zones would be ideal for a gradual transition (Smith, Xia, Galatz, Genin, & Thomopoulos, 2012). Good achievements for ACL reconstruction were delivered by Fan et al., who wrapped a microporous silk mesh around a silk cord and thereby created a silk scaffold. These scaffolds were seeded with MSCs and tested in pigs. In vivo, MSCs proliferated well and showed reliable differentiation into fibroblasts (Fan, Liu, Toh, & Goh, 2009).

In a study published by Kokubu et al., adipose-derived stem cells (ACs) were transplanted into an Achilles tendon injury at the early stage of tendon regeneration in a mouse model. ACs proved to modulate inflammation and initiate vascularization. Furthermore, they could prevent undesirable ectopic bone formation (Kokubu et al., 2020).

2.3.3. Growth Factors

Growth factors are the second main pillar of tissue engineering (A. Moshiri et al., 2013). As they play a regulating role in all cellular processes, they have great potential for regeneration purposes. Anyhow, their short half-lives create challenges for their safe application (Mitchell, Briquez, Hubbell, & Cochran, 2016). When administered free of a suitable delivery system, their uncontrolled release can constitute risks (Silva et al., 2017).

Finding new strategies that guarantee stability and support a controlled activity of growth factors is essential (Font Tellado et al., 2018). Scaffolds may act as a reservoir and guide growth factors release at a controlled rate. This way, a monitored influence on tissue formation can be exerted (Santo, Gomes, Mano, & Reis, 2013). Biphasic silk-fibroin scaffolds were tested as a delivery platform for growth factors (TGF- β 2 and Growth/differentiation factor 5) in enthesis regeneration. Coupled with heparin-functionalization, they proved to be suitable for continuous growth factor release. In *in vitro* experiments, the growth factor loaded

scaffolds guided adipose-derived mesenchymal stem cells (AdMSCs) in the direction of functional enthesis regeneration (Font Tellado et al., 2018).

2.3.4. Scaffolds

The third main pillar of tissue engineering are scaffolding materials. Scaffolds utilized for enthesis regeneration have to meet up with certain requirements. They should promote cell adhesion and growth, and thereby direct the formation of the regenerative tissue (Sahoo, Teh, He, Toh, & Goh, 2011). More precisely, since the scaffold must replace the ECM during the healing episode, mechanical strength is essential. It should support cell invasion and interaction and allow ECM disposition. In order to enable cell colonies to survive, a sufficient transport of gases and nutrients through the scaffold must be guaranteed. Biocompatibility and gradual biodegradability are further essential features (Font Tellado et al., 2015). To support ideal tissue regeneration, a scaffold should mimic the native structure of the ECM (J. A. Cooper, Lu, Ko, Freeman, & Laurencin, 2005). It was shown that the scaffold structure and in particular the scaffold surface are of key importance for cell attachment, interaction, ECM production, and proliferation (Font Tellado et al., 2015).

On the osteotendinous junction, it is especially difficult to find an appropriate replacement because it has a multi-zone structure. However, since the enthesis function is closely linked to its' structure, an ideal scaffold needs to mimic the zonal construction (Qu, Mosher, Boushell, & Lu, 2015).

Generally, materials used to fabricate scaffolds can be of natural or synthetic origin. Also, biologic materials such as acellularized cadaveric tissues have been used. Natural-origin materials include collagen, elastin, fibrin, and silk. Examples of synthetic materials are polypropylene, carbon, and hydroxyapatite (Ali Moshiri & Oryan, 2013).

Identifying the right material for a certain application is challenging. Silk has demonstrated its' potential in ACL reconstruction (Altman et al., 2002; Altman, Horan, Weitzel, & Richmond, 2008). Due to its natural mechanical properties close to those of ligaments and tendons, it is especially suited to replace these tissues (Font Tellado et al., 2018). During the extended period of biodegradation, the newly formed tissue has enough time to regain mechanical strength (Teuschl et al., 2016). Unlike synthetic polymers, silk has not shown immunological responses during degradation. This is due to the fact that silk is a protein and thereby degrades into peptides (Cao & Wang, 2009). A disadvantage of silk as a biomaterial is that it has suboptimal cell recruiting qualities (Shen et al., 2012). Researchers have approached this problem in different ways. Qian et al. have combined the mechanical properties of silk with the advantages of collagen, as a material with good biocompatibility and fabricated a combined scaffold for ACL reconstruction. Improved healing of the osteotendinous junction in rabbits was shown (Qian et al., 2019). Another approach was to refer to the layer of the ligament-to-bone interface by creating a triphasic scaffold. Additionally, specific cells were seeded into each phase. This strategy also showed promising results for the interface regeneration in a rabbit ACL model (Li et al., 2016).

In these studies, silk has proven to be a biomaterial with a lot of potential for ligament, tendon, and tendon-to-bone interface reconstruction. Further tests regarding the application of silk for the reconstruction of these tissues are well-founded.

A functional scaffold remains the foundation of all experimental approaches regarding tendon-to-bone interface healing. Although growth factors play a role in all healing processes, their utilization for a multi-zonal interface may prove difficult (Calejo et al., 2019). For stem cells, a challenge can be to find a suitable delivery system that controls the distribution of biological molecules regarding time, place, and amount. Uncontrolled distribution of molecules can affect all cells present at the healing site and lead to undesired responses

and a poor outcome (Bianco, Moser, Galatz, & Huang, 2019). Overall, a scaffold-only approach to support the natural healing capacity is preferable. Scaffolds are easily accessible and employable. This leads to the assumption that the application of a scaffold only might prove to be the best option for the regeneration of the tendon-to-bone interface.

2.4. PREVIOUS EXPERIMENTS AND AIM OF THIS STUDY

The special challenge is to create a scaffold that helps to regain the gradual transition zones of the enthesis while promoting cell migration and tissue ingrowth.

Previous to this study, two different types of biphasic silk-fibroin scaffolds with a difference in their transition zone were designed (Font Tellado et al., 2017). Two phases featuring different pore alignments were designed that should mimic the sides of the tendon-to-bone interface. Anisotropic pore alignment was used for the tendinous side and isotropic at the bony attachment, the connection of the two sides was achieved through a transition zone that differed in the two types of silk-fibroin scaffolds. These scaffolds were tested *in vitro* and showed promising results regarding cell attachment and proliferation (Font Tellado et al., 2017).

As a continuation of the *in vitro* study by Font et al., biphasic silk-fibroin scaffolds were implanted into patella tendon-to-bone enthesis defects in rats to be tested *in vivo*. Samples were harvested after four and twelve weeks, a control was harvested from the contralateral side. The aim of the present study was to perform a radiologic and histological evaluation of the *in vivo* enthesis regeneration using these biphasic silk-fibroin scaffolds.

2.5. EVALUATION METHODS

As mentioned, ectopic bone formation can develop during the healing process of soft tissue (Davis et al., 2011). In order to identify and evaluate the amount of heterotopic ossification, μ CT was conducted on all samples.

Subsequently, all samples were processed for histological evaluation. Aspects such as cell density and alignment, vascularity, as well as collagen alignment were examined and compared between the experimental groups and native tissue. Histopathological assessment was performed following the scoring system formulated by Watkins et al. (Watkins, Auer, Morgan, & Gay, 1985).

2.6. HYPOTHESIS

Preceding this study, the following four hypotheses were phrased.

1. The implantation of silk-fibroin scaffolds into an enthesis defect leads to less ossification in the tendon compared to the control groups.
2. The implantation of silk-fibroin scaffolds into an enthesis defect leads to interface healing with histological properties similar to a native enthesis.
3. The different interface structures of the silk-fibroin scaffold have an influence on the occurrence of ossification during healing and the regain of the histological characteristics of a native enthesis.
4. Silk-fibroin is a good material for enthesis regeneration.

3. MATERIAL AND METHODS

3.1. SCAFFOLD DESCRIPTION

In this study, porous, biphasic silk-fibroin scaffolds were used to treat patellar enthesis defects in rats. The scaffolds have been previously fabricated, characterized, and reported elsewhere (Font Tellado et al., 2017). In brief, the scaffolds were highly porous, with the majority of pores in the range of 100–300 μm . The scaffolds featured multizone-mimicking structures, that is a bony part, an interface, and a tendon part were present. The scaffold's pore alignment was anisotropic at the tendon/ligament side and isotropic at the bone side. Two different types of scaffolds were tested *in vivo* and analyzed here. They featured distinctive structures at the bone-to-tendon transition site. Two different fabrication protocols resulted in two scaffolds with a difference in their transition zone. The scaffold named “A” featured an abrupt transition between the bony and the tendon part. Conversely, the scaffold termed “B” featured an interconnected and thus smoother transition zone. In Figure 5 the morphology and structure of the two studied scaffolds in a μCT reconstruction (figure part “A”) and electron microscopy (figure part “B”) is shown. In figure part “A” the left two pictures show the whole scaffolds whereas the right picture shows the pore morphology at the transition zone. A more detailed look on the pores is given in figure part “B” (Tellado, 2018). This figure has been reproduced with permission from Mary Ann Liebert from Font Tellado et al., 2017 for this thesis.

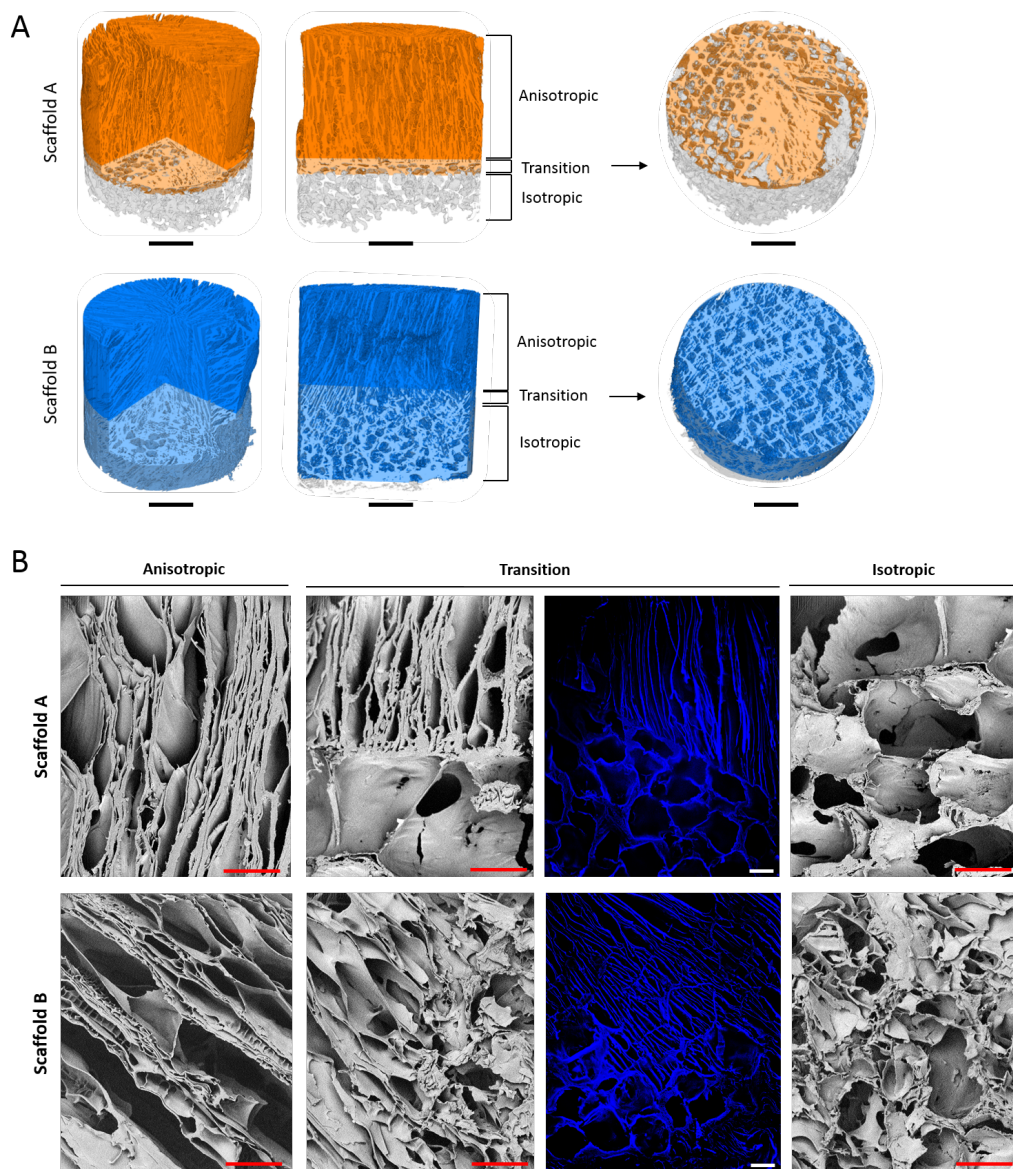


Fig. 5: Structure of biphasic silk-fibroin scaffolds. μ CT reconstruction (A), field emission scanning electron microscopy and fluorescent microscopy (B) illustrating the morphology of the areas with anisotropic and isotropic porosity and the transition zone. Scale bars = 300 μ m. Reprinted with permission from Mary Ann Liebert from (Font Tellado et al., 2017).

3.2. PATELLAR ENTHESES MODEL

A rat patellar enthesis model was developed for this study in order to test the potentialities of the developed scaffolds for *in vivo* enthesis repair. For this, the animal study and protocols used were approved by the Institutional Animal Care and Use Committee of the Mayo Clinic

(Rochester, MN, USA, Protocol Number A00002479-17). Previously, the patellar enthesis model has been published (Peniche Silva et al., 2022). Sprague Dawley rats (male, ~400g, Charles River Laboratories, Wilmington, MA, USA) were used. After acclimatization of the animals to the animal facilities, surgery was performed. For this, rats were anesthetized using isoflurane (~4%, O₂ flow of 1.5–2.0 l/min) followed by Buprenex (0.6 mg/kg) and cefazolin (50 mg/kg) that were administered subcutaneously. Before starting surgery, the right leg was shaved and disinfected with iodine. Next, the foot was secured to the operation table, in the desired position using tape. A longitudinal incision from the distal femur to the proximal tibia was made. The patellar tendon was exposed and subsequently detached from the tibial insertion using a scalpel. At the tibial insertion side, a defect in the bone was created using a gigli saw. Predetermined treatment was applied following the description provided hereafter (3.3.) and the tissue defect was closed by suturing the incision in layers. After the surgery, the animals were placed back in their cages and carefully monitored for recovery. The animals were allowed to move freely. No restriction or immobilization was performed. Analgesia was performed following routine, established protocols at the animal facility. The wounds were inspected daily for the first 5 days.

3.3. SCAFFOLD IMPLANTATION AND STUDY DESIGN

A total number of 37 samples of rat patella entheses were analyzed in this work. Five groups were evaluated, that is an empty defect, a transversal tendon cut, a collagen treatment, and two groups treated with silk-fibroin scaffolds. In the control group, an empty defect was used. In this group, no treatment was performed. Instead, the patellar tendon was sutured back over the created bony defect. Similarly, in the transversal tendon cut, no treatment was performed. Here, a transversal cut at the tendon near the enthesis was performed without damaging the bony structure. In the next three groups, an implantable 3D material was used as treatment. One of them included a commercially available collagen sponge. The other two groups, that are the relevant study groups, comprised the silk-fibroin scaffolds. One used the scaffolds featuring an abrupt transition zone (“A”)

and the other one the scaffold with an interconnected transition zone (“B”). In these groups, the silk-fibroin scaffolds were oriented with the bony part to the tibial plateau and the tendon part towards the patellar tendon. The scaffolds were secured into the defect using sutures.

Samples were harvested four and twelve weeks after surgery.

Furthermore, a native enthesis was harvested from the contralateral side.

3.4. MICRO-COMPUTED TOMOGRAPHY (μ CT)

Explanted samples of rat patella tendons were fixed in 4% paraformaldehyde (PFA) over a period of 24 hours. Afterwards, they were rinsed with phosphate-buffered saline (PBS) and stored in 70% ethanol. The scanning of all samples was performed in this 70% ethanol solution using a μ CT (Skyscan 1176, Bruker, Kontich, Belgium) at 90 kV, 277 μ A with a 0.1 mm Cu filter. The acquisition of image projections happened at a resolution of 35 μ m every 0.7° rotation step over 360° rotations around the vertical axis. For the processing of CT images, the volumetric reconstruction software, NRecon (version 2.0.4., Bruker, Kontich, Belgium) was used. Analysis for the quantification of mineralized nodules within the regenerating niche was performed with the CTAnalyser software (Version 1.13., Bruker, Kontich, Belgium). Briefly, a region of interest (ROI) was selected by cutting out the bone that belongs to the patella or the tibia in all the μ CT layers, as illustrated in Figure 6. These bony areas were excluded from the calculation of the bone mass. Thereby, it was guaranteed that only the ossification in the tendon area was integrated into the calculation. Then, the ROI (green) for the calculation was selected as shown in Figure 7. The Global threshold of 90 to 255 was applied for all samples, representing the mineralized nodules within the regenerating niche.

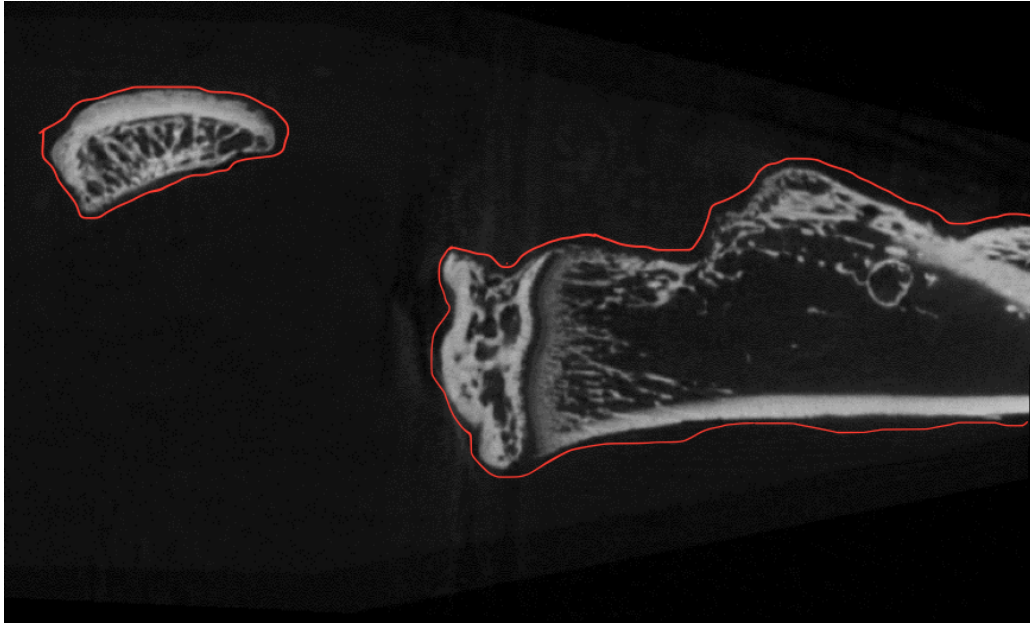


Fig. 6: Selection of bone belonging to the patella and the tibia in CTAnalyser.

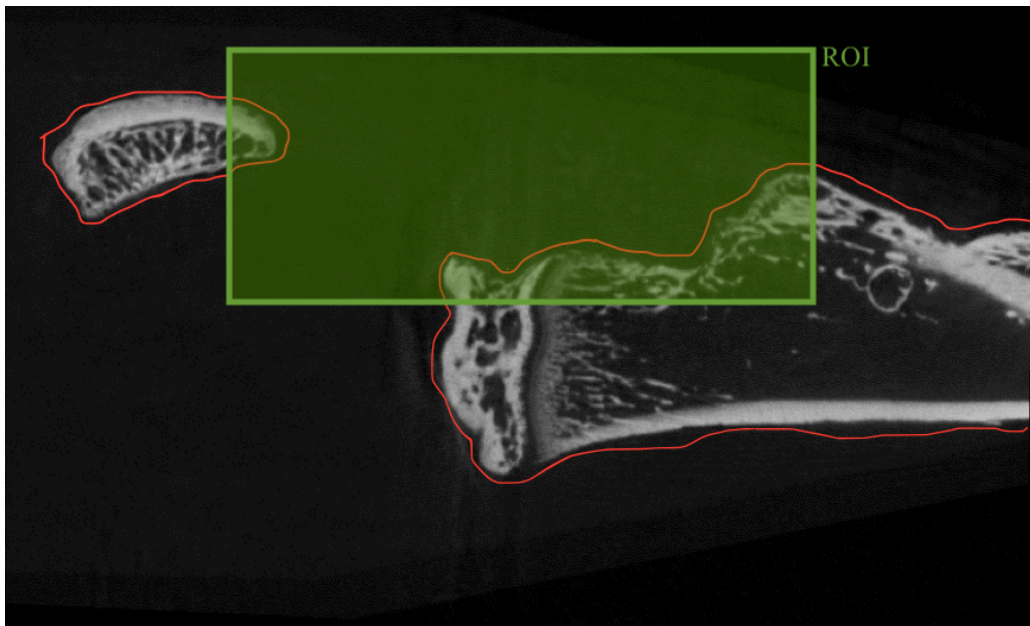


Fig. 7: A ROI that was considered for the calculation of the bone mass was selected in CTAnalyser.

3.5. HISTOLOGY: DECALCIFICATION

To section bone samples for histology, the samples needed to be decalcified. For this purpose, 10% Ethylenediaminetetraacetic acid (EDTA) solution was used. The solution was prepared by dissolving EDTA disodium salt in distilled water and adjusting the pH to 7,4. For this, a

titration was performed with sodium hydroxide (NaOH) 50%. As soon as all particles were solved, the solution was considered ready to use.

Samples were placed in the 10% EDTA solution for 14 days. A solution change was performed every two to three days. To expedite the decalcification, the solution was always kept in motion using a magnetic stirrer. For determining the endpoint of the decalcification, μ CTs and macroscopic examination were performed. To stop the decalcification process, samples were washed in PBS, put back in 70% ethanol and stored at +4°C until further analysis.

3.6. HISTOLOGY: PARAFFIN EMBEDDING

Dehydration and paraffin infiltration were performed with the Shandon Excelsior Tissue Processor (Thermo Fisher Scientific Inc., Waltham, USA). Then paraffin blocks were produced with the Tissue Tec (Sakura Finetek Europe B.V., Alphen aan den Rijn, Netherlands). The correct placement of the samples in the paraffin block was of major importance to secure the obtention of adequate sections. Therefore, care was taken to position all the samples equally inside the histology cassettes to ensure comparable sections. The blocks were stored at +4°C until further sectioning.

3.7. HISTOLOGY: SECTIONING

As a preparation for the sectioning, the paraffin blocks were put on ice or in a freezer for 30 min. Freezing improved the quality and the durability of the sections. Thereafter, sections of 7 μ m thickness were sliced using the LEICA RM 2165 microtome (Leica Biosystems Nussloch GmbH, Nussloch, Germany) and placed on Menzel-Gläser SUPERFROST PLUS microscope slides (Thermo Fisher Scientific Inc., Waltham, USA).

3.8. HISTOLOGY: STAINING OF TISSUE SECTIONS

Prior to the staining, the sections were deparaffinated and rehydrated according to the following protocol:

1. Roti-Histol for 8 min
2. Roti- Histol for 8 min
3. 100% Ethanol for 5 min
4. 90% Ethanol for 5 min
5. 70% Ethanol for 5 min
6. 50% Ethanol for 5 min
7. distilled water for 2 min

3.8.1. Hematoxylin-Eosin Staining

Hematoxylin-Eosin is a standard method in histology to stain nuclei and basophilic substances blue and acidophilic components red. The staining was performed according to the following established protocol by (Mullisch & Welsch, 2010).

1. Stain with hem alum solution acid acc to Mayer for 5 min
2. Rinse in distilled water
3. Blue in running tap water for 15 min
4. Wash in distilled water for 2 min
5. Counterstain with Eosin Y solution 0,5% in water for 3 min
6. Wash in distilled water for 1 min

3.8.2. Masson-Goldner-Trichrome Staining

The Masson-Goldner-Trichrome is a specific staining for connective tissue.

It stains nuclei dark brown, cytoplasm and muscle red, erythrocytes orange and connective tissue green. The staining was performed according to the protocol provided by the manufacturer (Carl Roth GmbH+Co. KG, Karlsruhe, Germany).

1. Iron hematoxylin solution to Weigert for 3 min
2. Flowing tap water for 10-15min
3. Stain with Goldner stain I (Ponceau-Fuchsin) for 5-10min
4. Rinse in Acetic acid solution 1%

5. Stain with Goldner stain II (Phosphotungstic acid- Orange G) for 1-3 min
6. Rinse in Acetic acid solution 1% for 30 sec
7. Counterstain with Goldner's stain III (Light green SF yellowish) for 2-5 min
8. Wash in Acetic acid solution 1% for 2-5 min

3.8.3. Picro-Sirius Red Staining

This staining is specific for collagen. Under polarized light, the alignment of collagen fibrils can be visualized (Schmitz, Laverty, Kraus, & Aigner, 2010). The staining was performed according to the following protocol previously described by Rittié (Rittié, 2017).

1. Stain in a 0,1% picrid acid-saturated sirius red solution (1 liter of Picrid acid solution 1,3% in water and 1mg of Direct Red 80) for one hour
2. Wash in two changes of acidified water (5ml acetic acid in 995ml of distilled water)

After concluding each staining, the slides were dehydrated in an alcohol series with ascending alcoholic intensity and mounted using Roti Histokitt (Carl Roth GmbH+Co. KG, Karlsruhe, Germany). The dehydration was performed according to the following protocol:

1. 50% Ethanol for 2 min
2. 70% Ethanol for 2 min
3. 90% Ethanol for 2 min
4. 100% Ethanol for 2 min
5. Roti- Histol for 5 min
6. Roti- Histol for 5 min

3.9. MICROSCOPY

Photomicrographs were taken at four and ten times magnification with BIOREVO BZ-9000 microscope (Keyence Corporation, Osaka, Japan). Slides stained with Picro-Sirius Red were analyzed using polarized light microscope IX 83 (Olympus Corporation of the Americas, Westborough, USA). Representative slides of every staining and group were obtained and evaluated.

3.10. STATISTICAL ANALYSIS OF μ CT

All results of the μ CT analysis were inserted into Microsoft Excel (Microsoft Corporation, Redmond, USA). Mean bone volume in percent and standard deviation in the experimental groups as well as native tissue control were calculated at both time points. Data were represented in bar charts using Microsoft Excel.

3.11. HISTOLOGICAL EVALUATION

Visual histological evaluation of cell density and alignment, vascularity, and collagen alignment was performed based on the score developed by Watkins et al. (Watkins et al., 1985).

Image processing was performed with Adobe Illustrator, Photoshop (Adobe Systems Software Ireland Limited, Dublin, Republic of Ireland) and Microsoft PowerPoint (Microsoft Corporation, Redmond, USA).

4. RESULTS

4.1. EXPERIMENTAL GROUPS

Table 1 illustrates the different treatments applied to the enthesis defect as well as the control groups. In addition, listed in table 1 are also the sample numbers analyzed by μ CT. Five experimental groups were included. The patella enthesis was either cut transversally or a tissue defect was created and either left empty, treated with one of the biphasic silk-fibroin scaffolds or with a collagen sponge. Four and twelve weeks after implantation the animals were sacrificed and the tissue comprising the enthesis areas was removed. In 4 rats the contralateral patella tendon was resected and used as a native tissue specimen. Following the μ CT analysis, all samples were processed for histology, including section staining and histologic evaluation.

Table 1: Experimental groups included in the study. Applied treatment and groups are listed as well as sample numbers used for μ CT evaluation.

Group	Treatment	Sample number n (time point in weeks) for μCT
Empty	Enthesis defect; No treatment	n (4) = 4 n (12) = 4
Cut	Transversal tendon cut; No treatment	n (4) = 4 n (12) = 4
Collagen	Enthesis defect; collagen sponge inserted	n (4) = 2 n (12) = 3
Silk abrupt	Enthesis defect; Silk Scaffold A (abrupt transition) inserted	n (4) = 4 n (12) = 4
Silk interconnected	Enthesis defect; Silk Scaffold B (interconnected transition) inserted	n (4) = 4 n (12) = 4
Control	Contralateral, native enthesis	n = 4

4.2. MICRO-CT ANALYSIS

Micro-CT was used to detect the presence or absence of ossification in the tendon area. Fig. 8 and fig. 9 give an overview of the percentage of bone in the patella tendon at 4- and 12-weeks, respectively. The mean bone volume is indicated in bone volume in percent (%) (bone volume in μm^3 /tissue volume μm^3). As there was a considerable higher amount of bone volume after twelve weeks, unequal scales on the y-axis are used for greater clarity. At both time points, the same control group, that is the native tissue was used as a reference. Data are represented as the mean \pm the standard deviation for each of the analyzed groups.

After four weeks, no significant difference between the experimental groups was detected. The empty group and the group with the tissue cut, which are representative of conservative treatment, showed very low mean levels of ossification. In both groups, little variation between the samples occurred. The collagen group showed a higher mean tendency of ectopic bone formation (0.11%). Anyhow, there was a high standard deviation in this group (0.11%). In the silk-fibroin scaffold groups, a relatively low mean level of ectopic bone formation was observed (0.0017% in the abrupt transition group and 0.02% in the interconnected transition group). Of note, it could be appreciated that the standard deviation was very low in the group with the abrupt transition (0.0015%) and only slightly higher in the group with the interconnected transition (0.017%). Moreover, the control group showed a low mean levels of ectopic bone formation (0.0017%) as well as a small standard deviation (0.0018%).

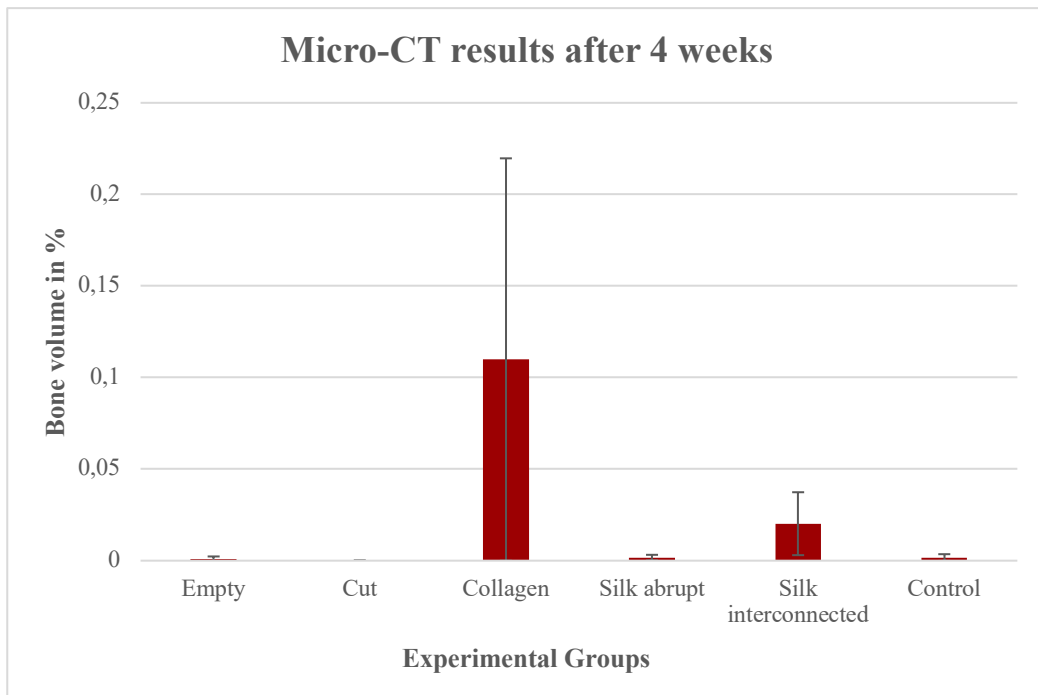


Fig. 8: Micro-CT results after 4 weeks; red columns display the mean bone volume of all samples within the same group. The black vertical line shows the standard deviation.

Twelve weeks after surgery, all experimental groups showed significantly higher mean levels of ectopic bone formation compared to the control group. Unexpectedly, the group with the empty entheses defect showed the lowest level of ectopic bone formation of all experimental groups (0.73%). Notably, in this group, a high standard deviation occurred (0.64%). In the group with the tissue cut the highest mean level of ossification was observed (1.65%). The third-highest amount of mean bone volume was found in the collagen group (1.45%). However, similar to the untreated defect group, there was a substantial standard deviation associated with this group (0.94%). The group treated with the silk-fibroin scaffold featuring an abrupt interphase transition resulted in the second-largest mean amount of ectopic bone formation (1.53%). In the silk-fibroin scaffold group treated with the interconnected transition the second-lowest level of ossification was detected (1.06%). Moreover, in this group the standard deviation was relatively low compared to the other experimental groups (0.4%).

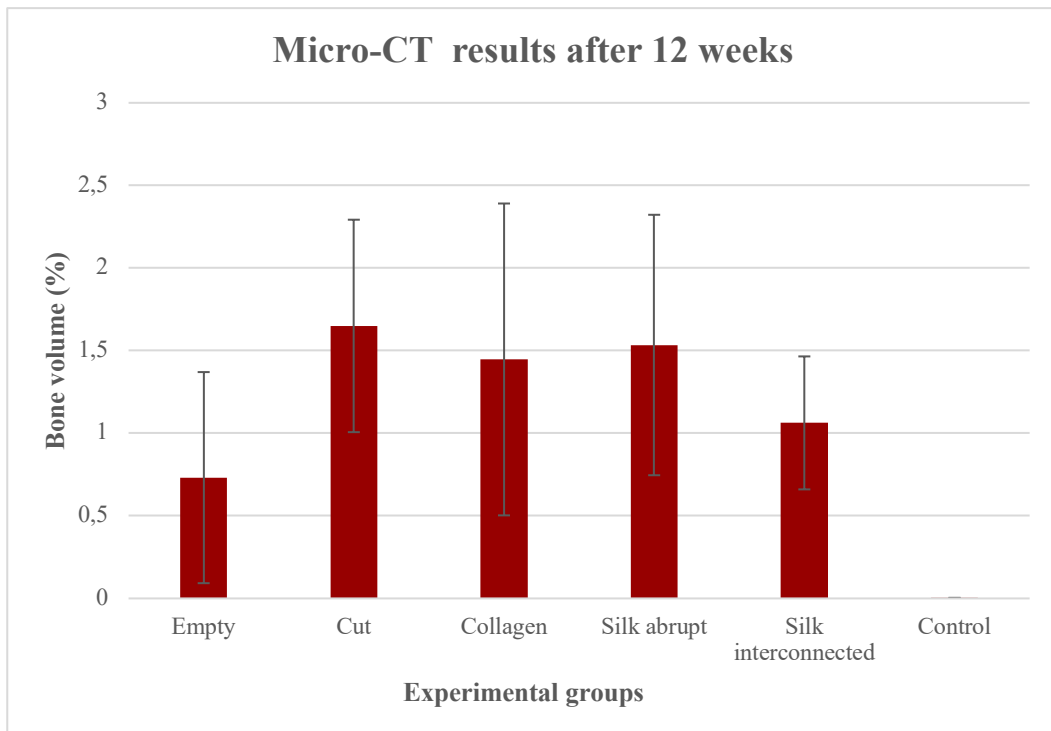


Fig. 9: Micro-CT results after 12 weeks; red columns display the mean bone volume of all samples within the same group. The black vertical line shows the standard deviation.

4.3. HISTOPATHOLOGICAL CHARACTERISTICS

4.3.1. Sample Numbers for Histology

Table 2 gives an overview of the slide numbers processed by each staining as well as the time points taken into account during the histological evaluation.

Table 2: Slide number used for each staining and time point.

Experimental Group	Slide number n (time point) in hematoxylin eosin staining	Slide number n (time point) in Masson-Goldner-Trichrome staining	Slide number n (time point) in Picro-Sirius Red staining
Empty	n (4) = 6 n (12) = 5	n (4) = 8 n (12) = 5	n (4) = 2 n (12) = 3

Cut	n (4) = 7 n (12) = 6	n (4) = 6 n (12) = 7	n (4) = 2 n (12) = 2
Collagen	n (4) = 5 n (12) = 5	n (4) = 5 n (12) = 4	n (4) = 2 n (12) = 3
Silk abrupt	n (4) = 6 n (12) = 6	n (4) = 5 n (12) = 9	n (4) = 2 n (12) = 3
Silk interconnected	n (4) = 5 n (12) = 5	n (4) = 6 n (12) = 7	n (4) = 3 n (12) = 3
Control	n (12) = 6	n (12) = 6	n (12) = 2

4.3.2. Cell Density and Alignment to the Longitudinal Axis

To analyze the cellularity present in each of the experimental groups, hematoxylin and eosin staining was conducted. This staining allowed us to identify the type of cells present in the specimens. Relevant features such as cell alignment and distribution were also evaluated.

Table 3 gives an overview over the cell density. A score was introduced to indicate the cellularity from low (+) to high (+++). Representative images are depicted in Figure 10.

In comparison to the control, all experimental groups showed an increase in cellularity at both time points. In the group with the empty tissue defect, the highest increase of cell density was detected. This was the case for both time points analyzed. In the tissue cut group and the group treated with collagen, a rise of the cell number was observed at both time points. No major difference between the cellularity at the two time points in these groups was distinguished. The experimental groups in which the silk scaffolds were applied, showed a vast increase of cell density after four weeks but a slight reduction after twelve weeks.

Looking at the cell alignment, it is important to note that the control group showed parallel cell alignment in the tendonous area.

Table 4 gives an overview over the obtained results. A score system was used to indicate the presence of aligned areas, from

unorganized (-) to organized (++) cell alignment. Representative slides are depicted in Figure 10.

After four weeks, the group with an empty entheses defect showed hardly any areas of aligned cells. In the other experimental groups, some areas with parallel cell alignment were detected. Still many areas of unorganized cell formations occurred.

After twelve weeks, areas with oriented cell alignment were found in all experimental groups.

Table 3: Cell density in entheses specimens harvested at 4- and 12-weeks post-surgery. Low cellularity is indicated by +, moderate cellularity by ++, and high cellularity by +++.

Group	Empty	Cut	Collagen	Silk abrupt	Silk inter-connected	Control
4 weeks	+++	++	++	+++	+++	
12 weeks	+++	++	++	++	++	+

Table 4: Cell alignment in tendinous part; Hardly any alignment detectable: -, alignment in few areas: +, organized alignment of tenocytes: ++.

Group	Empty	Cut	Collagen	Silk abrupt	Silk inter-connected	Control
4 weeks	-	+	+	+	+	
12 weeks	+	+	+	+	+	++

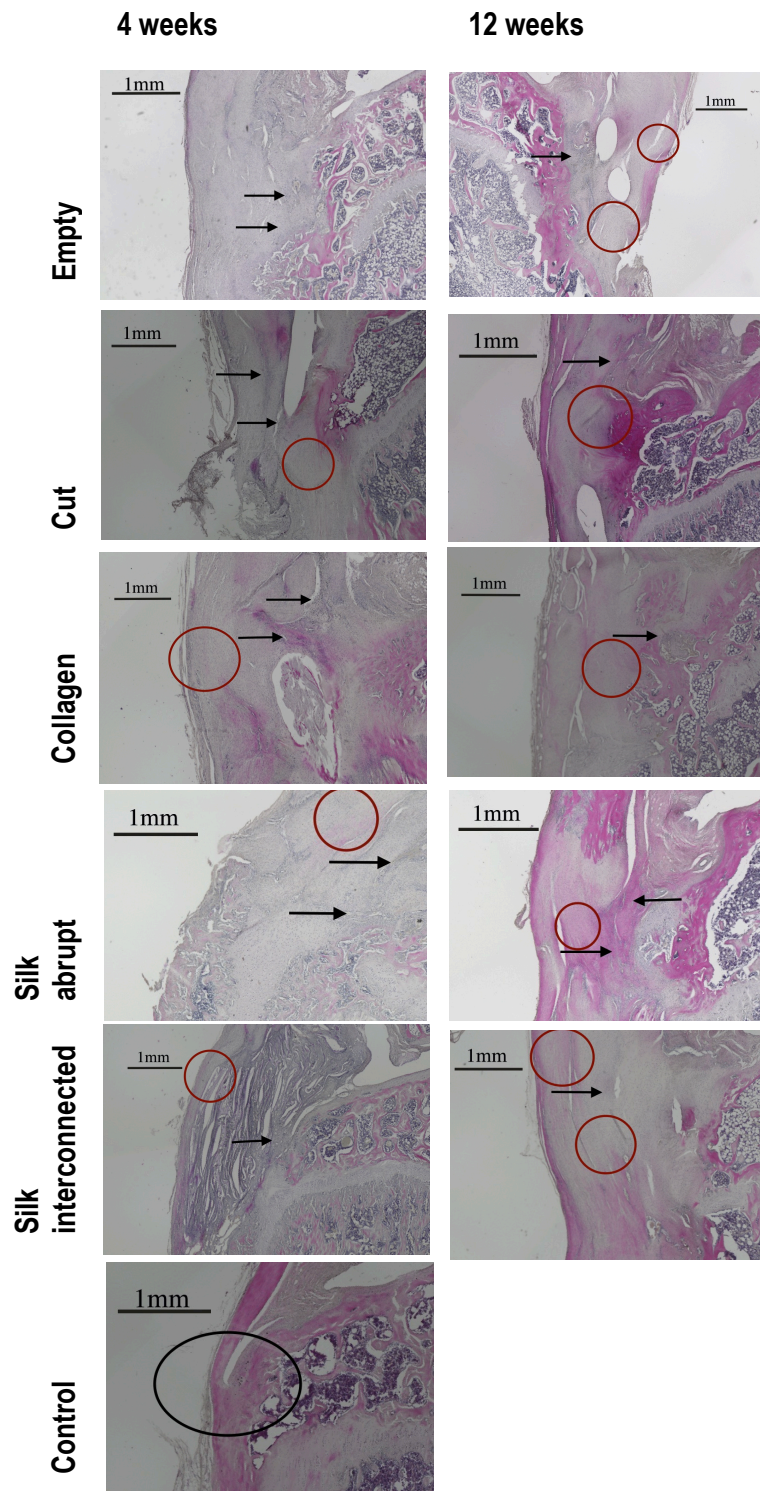


Fig. 10: Representative images of the specimens stained with Hematoxylin and Eosin. Native enthesis in the control group is indicated by a black oval. Black arrows indicate areas with high cellularity. Red circles indicate areas with parallel cell alignment.

4.3.3. Vascularity

The presence of vascularity in the explanted samples was evaluated using histological slides stained with Masson-Goldner-Trichrome.

Table 5 gives an overview of the obtained results using a score from (-) indicating no blood vessels to (++) for several blood vessels. Representative slides are shown in Figure 11.

In all experimental groups blood vessels were located.

After four weeks, less blood vessels were found in the group with the empty tissue defect and the tissue cut compared to the remaining groups.

After twelve weeks, in all experimental groups apart from the group with the empty defect, several blood vessels were identified in the osteotendinous junction.

In both groups treated with the silk-fibroin scaffolds, several blood vessels were detected at both time points.

Table 5: Vascularity in harvested enthesis specimens: few blood vessels in enthesis are indicated by -, some blood vessels by +, and several blood vessels by ++.

Group	Empty	Cut	Collagen	Silk abrupt	Silk inter-connected	Control
Time Point						
4 weeks	+	+	++	++	++	
12 weeks	+	++	++	++	++	-

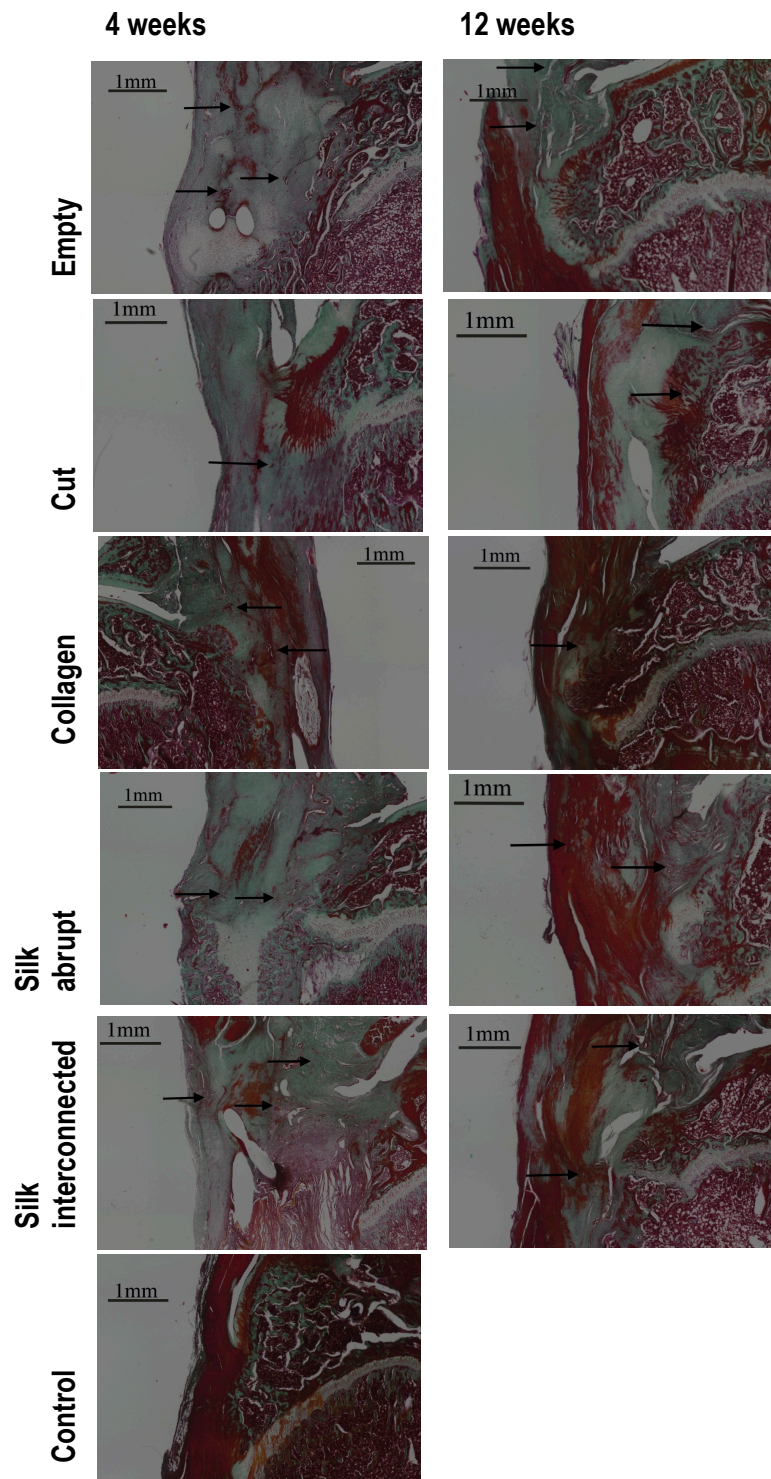


Fig. 11: Representative slides for each group stained with Masson Goldner Trichrome. Black arrows indicate the presence of blood vessels.

4.3.4. Collagen Alignment

To examine the collagen alignment, the Picro-Sirus Red staining was conducted.

In the native enthesis, an organized transition zone was observed. Parallel aligned collagen fibers were identified, attached at the bony insertion side.

Table 6 gives an overview of the obtained results for all investigated groups. Similarly, a scoring system was used here to indicate the levels of collagen fiber organization from a few organized areas (-) to organized tendon-to-bone junction (++). Representative slides are pictured in Figure 12.

After four weeks, no areas of parallel collagen alignment were identified at the insertion side of the groups: empty tissue defect, collagen sponge treatment, or silk-fibroin scaffold with the abrupt transition. Conversely, in the group with the tissue cut and the silk-fibroin scaffold with the interconnected transition, parallel organized collagen fibers were detectable in some areas.

After twelve weeks, the group with the empty tissue defect and the group treated with a collagen sponge still appeared unorganized in all tissue areas analyzed. In the group with the tissue cut, some areas with parallel alignment were spotted. In both groups in which silk scaffolds were applied, several areas with organized collagen fibers were identified.

Table 6: Collagen alignment in harvested enthesis specimens: few organized areas indicated by -, several organized areas by +, and organized tendon-to-bone junction by ++.

Group	Empty	Cut	Collagen	Silk abrupt	Silk inter-connected	Control
4 weeks	-	+	-	-	+	
12 weeks	-	+	-	+	+	++

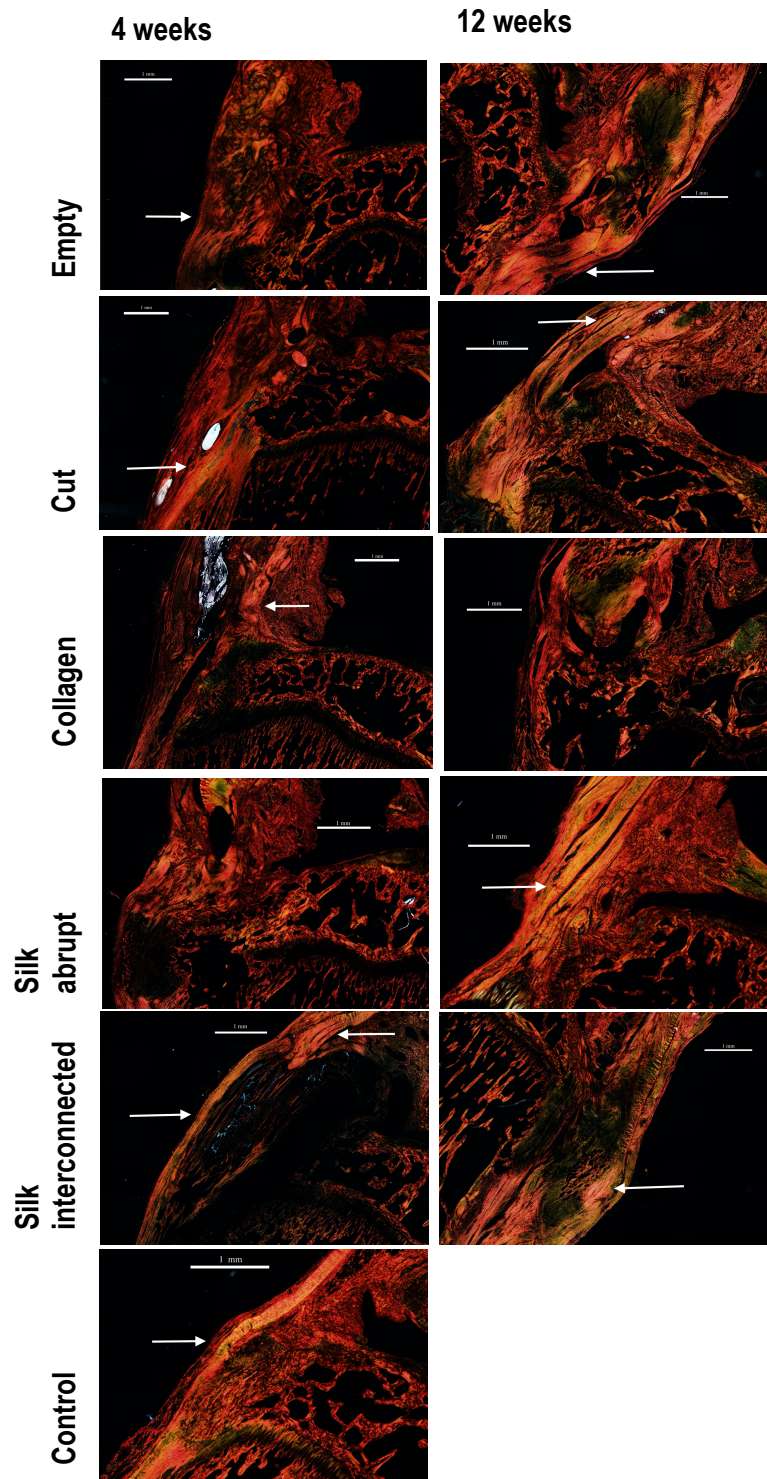


Fig. 12: Representative slides for each group stained with Picro-Sirius Red. White arrows indicate areas with organized collagen alignment.

5. DISCUSSION

The self-healing capacity of the tendon-to-bone insertion after enthesis injuries is low. Thus, research regarding the integration of tendon-to-bone junction is of high clinical interest. Most of the current treatments fail in promoting sufficient regeneration of the transition zone. This results in high re-rupture rates and morbidity at the implantation site (Font Tellado et al., 2018).

Based on this knowledge, previous to this study two sorts of biphasic silk-fibroin scaffolds were developed and tested *in vitro* using adipose-derived mesenchymal stem cells. In these studies, silk scaffolds showed great potential in guiding cellular differentiation (Font Tellado et al., 2017; Font Tellado et al., 2018). The aim of the current study is to histologically evaluate the healing capacity of the previously developed biphasic silk-fibroin scaffolds *in vivo* in a rat patella enthesis tendon defect model. Additionally, the occurrence of heterotopic ossification in the regeneration zone was investigated by means of μ CT.

5.1. STUDY GROUPS AND TREATMENT

Five study groups were created which are mentioned in chapter 4.1. The following paragraph gives a short summary.

In the first group, an enthesis defect was created but left untreated and the patella tendon was sutured over the created bony defect.

In the second group, the tendon was cut transversally, no intervention was further performed, and the bone remained uninjured. This imitated a tendon cut with an approximation of the two ends.

In the third group, an enthesis defect was created and a collagen sponge was inserted as treatment. Collagen, a natural origin material that serves as a promoter of tendon regeneration, has been tested in multiple studies (Bi, Shi, Liu, Guo, & Yan, 2015; D. Lu, Yang, Zhang, & Xiao, 2018; Muller, Durselen, Heisterbach, Evans, & Majewski, 2016; Qian et al., 2019). As collagen biomaterials have been proved as supportive in enthesis regeneration, the comparison of this material to silk-fibroin scaffolds is especially interesting.

In the last two groups, the biphasic silk-fibroin scaffolds were tested. Scaffold type A consisting of a solid fibroin layer featured an abrupt transition at the interphase while scaffold type B was characterized by an interconnected transition zone between the areas of isotropic and anisotropic porosity (Font Tellado et al., 2017). Both scaffolds were applied as treatment to the enthesis defect.

Samples were harvested at four and twelve weeks after surgery. A native enthesis was harvested from the contralateral side that served as control. All study groups were compared in terms of ectopic bone formation present at the regenerated tissue site. In addition, histopathological characteristics were evaluated.

5.2. MICRO-CT ANALYSIS

Micro-CT analysis was performed to measure the occurrence of ectopic bone formation in the regenerated area. Ectopic bone formation is a common problem during the regeneration of soft tissue (Davis et al., 2011; Xu et al., 2018; Zhang et al., 2020). It can lead to an elongated healing process and higher morbidity (Davis et al., 2011).

After four weeks, little to no ossification was detected across the studied groups except for the collagen-treated group. In this group, a large ectopic bone formation was detected, although no statistical significance could be shown when a comparison among the groups was performed. Thereafter, at twelve weeks, all study groups showed significantly higher levels of ectopic bone formation compared to the native tissue control. Consequently, these results may suggest that the produced tissue trauma caused heterotopic ossification. Additionally, the fact that the amount of heterotopic ossification increased significantly between the first and second time point, suggest that heterotopic ossification is likely to occur between one to three months after trauma. This would happen during the proliferation and remodeling stage of the healing process (Schneider et al., 2018). This concurs with the assumption that heterotopic ossification forms between six to twelve weeks after trauma and reaches maturation between 12 to 24 weeks (Board et al., 2007; Hurlimann et al., 2017). Still, Craven and Urist have shown a significant reduction in the occurrence of

heterotopic ossification in a rat model where radiation was performed in the first week compared to when radiation was performed in the second week in a demineralized bone matrix was implanted into muscle (Craven & Urist, 1971). Hence, morphogenetic initialization is likely to happen within the first week.

The abrupt transition group, similarly to the transversal tendon cut, and the group that was treated with a collagen sponge showed the largest mean amounts of ossification after twelve weeks. In the interconnected transition a lower mean percentage of ossification developed. The fact that the group treated with a collagen sponge developed a rather high amount of ossification at both time points is especially interesting. A study, published by Bi et al., in which silk-collagen scaffolds were used for ACL reconstruction, indicates that tendon-to-bone healing in the scaffold group was superior to the autograft group. When comparing this study to our findings, it is important to consider that Bi et al. reported mineralization in the bone tunnel of the ACL graft as a sign of enhanced tendon-to-bone healing (Bi et al., 2015). Thus, it can be assumed that collagen enhances the mineralization in the transition zone. This may be beneficial for the integration of the transition zone between bone and mineralized fibrocartilage. However, bone formation that exceeds the mineralized area of the tendon-to-bone junction is considered pathological (Zhang et al., 2020). Considering our results for the collagen sponge and those of Bi et al., it could be concluded that collagen may not be an adequate material for the enthesis regeneration, but rather for the bony end of the enthesis. A difference in the occurrence of ectopic bone between silk-fibroin scaffold type A (abrupt transition) and type B (interconnected transition) was noticeable. Even though no significant differences were detected, scaffold type A with the abrupt transition showed the higher mean amount of heterotopic ossification after twelve weeks. These results seem to verify the third hypothesis postulated in this study, that the scaffold structure has an influence on the occurrence of ossification.

As the exact etiology of ectopic bone formation is yet to be found, it is especially difficult to prevent it. Various triggers, such as injury, inflammation, or hypoxia have been associated with the differentiation of

progenitor cells into cartilage or bone (Davis et al., 2011; Kokubu et al., 2020; Zhang et al., 2020). Currently, bisphosphonates, NSAIDs, and radiation are used to prevent heterotopic ossification (Xu et al., 2018). However, neither of the above-mentioned have proved to be completely effective in preventing heterotopic ossification. They are also not successful in treating heterotopic ossification once it has occurred. Surgical excision is a therapy used for undesired ossification, but the tissue trauma can cause recurrence (Zhang et al., 2020). To find a scaffold that leads to less ectopic bone formation in the tendon was one aim of this study. As there was no significant difference between the studied groups, the first hypothesis “The implantation of silk-fibroin scaffolds onto an enthesis defect leads to less ossification in the tendon compared to the control groups.” could not be confirmed. Anyhow, the interconnected silk-fibroin scaffold showed promising results and further tests are conceivable. *In vivo* tests of this scaffold in combination with the treatments that are currently used to prevent ossification would be especially interesting. In a recent study, the effect of adipose-derived stem cells on ectopic bone formation, inflammation and neovascularization was evaluated in tendinopathy (Kokubu et al., 2020). A reduction of ectopic bone formation was found in the ASC group. A study that investigates on the effect of ASCs applied on the biphasic silk-fibroin scaffolds could be considered, as well.

5.3. CELL DENSITY AND ALIGNMENT PARALLEL TO THE LONGITUDINAL AXIS

The native tissue obtained from the contralateral site demonstrated that the native enthesis has a low cell count. The enthesis is divided into four zones that contain different cell types. The tendinous area with aligned tenocytes, the non-mineralized fibrocartilage with fibrochondrocytes, the mineralized fibrocartilage containing hypertrophic chondrocytes and the bony part with osteoblasts, osteoclasts and osteoblasts (Font Tellado et al., 2015). Especially on the tendinous side of the enthesis, an area with low cell density and a high proportion of ECM occurs (Docheva et al., 2015). Here, tenocytes are the producer of the ECM, mainly consisting of

collagen type I, elastin, glycoproteins, and proteoglycans (Wu et al., 2017). The high proportion of ECM supports the extraordinary function of the enthesis as a carrier of muscular work onto the bone (H. H. Lu & Thomopoulos, 2013; Schneider et al., 2018). Mechanical stimulation enhances the production of ECM (Nourissat, Berenbaum, & Duprez, 2015).

All study groups showed an increase in the cell number when compared to native tissue at both time points. A high cell density was observed mainly at four weeks after surgery. This is a typical development for the proliferation stage during which macrophages release growth factors and induce cell migration (Schneider et al., 2018). The proliferation stage is followed by the remodelling stage that starts four to eight weeks after injury and can last up to one year. Typical for this phase is that collagen type I is synthesized and cell density decreases (Voleti et al., 2012). Correspondingly, the cell density in most experimental groups was alleviated between the first and second time point. During the remodelling stage, tenocytes start to orient in the direction of the mechanical stress (Schneider et al., 2018). Fibrils of collagen are responsible for the tendon's robustness towards tension. Proteoglycans determine the viscoelasticity of the tendon. Together these components enable the tendon to be the main transmitter of force from the muscle onto the bone (Docheva et al., 2015).

In the group with a tendon defect without treatment, larger cell numbers were apparent at both time points. This could indicate that a large tendon defect leads to further inflammation and an irregular healing procedure.

In the two scaffold groups, the cell density seems to be higher after four weeks than after twelve. The ability of the cells to penetrate the scaffold is decisive in the first stage of inflammation and the initialization of healing. Often, this is a problem related to biomaterials used as scaffolds in tissue engineering (Font Tellado et al., 2015). Providing evidence that highly porous silk-fibroin scaffolds promote cell migration and thereby integration is a promising achievement of this study. Moreover, the reduction of cell density after twelve weeks can be recognized as a sign that silk-fibroin

scaffolds stimulate the natural healing capacity and restructuring during tendon regeneration.

After four weeks, only the group with the empty patella tendon defect showed inferior alignment in comparison to the other groups. At twelve weeks after implantation, areas of parallel cell alignment were seen in all study groups. The fact that areas of longitudinally orientated cells were identified in both groups treated with silk-fibroin scaffold is very promising, as it implicates that the ECM in these areas featured correct orientation of the fibers.

Still, areas featuring unorganized cell formations were observed. As the remodelling phase may take up to one year, it can be expected that these areas will arrange themselves to the axis of stress during that phase. Therefore, times of observation longer than 12 weeks after treatment may be necessary for enthesis injury models.

5.4. VASCULARITY

Generally, mature tendons are seen as sparsely vascularized and their nutrition is based on diffusion from the paratendon (Ahmed, Lagopoulos, McConnell, Soames, & Sefton, 1998; Gelberman, 1985; Schmidt-Rohlfing, Graf, Schneider, & Niethard, 1992). The paratendon is a tissue shield wrapping the tendon that allows movements in the surrounding tissue (Hoffmann & Gross, 2006). The blood supply on the osteotendinous junction is assured through the bone, the muscle, and the paratendon. Yet, the enthesis itself is seen to be avascular (Wu et al., 2017). In line with this, no blood vessels were found in the native enthesis tissue.

The relevance of proliferative vascularisation in tendons during healing is yet to be clarified. While chronic hypervascularity is regarded as a cause of pain and not as evidence of repair during tendinopathy, vascularisation has been claimed as an essential part of tendon healing after an acute injury (Fenwick et al., 2002). The supply of nutrients, cells, and oxygen is ensured via blood vessels in this phase (P. Sharma & Maffulli, 2006). In the early stage of tendon healing, angiogenesis is initialized by growth factors, such as VEGF, bFGF, TGF- β , EGF and PGFG (Bidder et al., 2000; Chang et al., 1998; Duffy et al., 1995; Kuroda et al., 2000; Wu et al., 2017).

The vascularization of tendon grafts during ACL repair has shown to be of key importance for tissue survival and long-term function of the graft (Fenwick et al., 2002; McFarland, Morrey, An, & Wood, 1986; Nikolaou, Seaber, Glisson, Ribbeck, & Bassett, 1986). Sufficient revascularisation can be expected after six weeks (Bosch & Kasperczyk, 1992; Kasperczyk, Bosch, Oestern, & Tscherne, 1993).

In all experimental groups, blood vessels were found at the osteotendinous junction. These results support the observation that neovascularisation is initialized during tendon healing (Wu et al., 2017). Especially, the biphasic silk-fibroin scaffolds supported vascularization at both time points. It substantiates the finding that silk-fibroin scaffolds support cell migration, as migration is known to be essential for angiogenesis, a relevant process for tendon repair. In fact, Kokubo et al. suggested that early neovascularization supports tendon repair and inhibits ectopic bone formation (Kokubo et al., 2020). The fact that the interconnected scaffold group showed low occurrence of ectopic bone formation and apparent blood vessel formation at both time points buttresses this assumption. However, in the group treated with a collagen sponge and the silk-fibroin scaffold group with the abrupt transition, neovascularisation and a higher level of ossification occurred.

Silk-fibroin scaffolds as well as the group treated with a collagen sponge showed more blood vessels after four weeks than the groups that were treated conservatively. This is a highly promising finding, as neovascularisation is an essential component in the early stages of tendon regeneration.

5.5. COLLAGEN ALIGNMENT

The correct orientation of collagen fibrils is a crucial element in the transmission of muscle strength onto the bone (Nourissat et al., 2015).

The collagen structure was visualized by staining with Picro-Sirius Red and examined under polarized light (Loppini et al., 2015).

In the native enthesis well organized, longitudinally oriented collagen fibers were identified that inserted at the osteotendinous junctions. This

observation is in line with that of Apostolakos et al. for native enthesis tissue (Apostolakos et al., 2014).

At four weeks, only the group with the transversal tendon cut and group treated with the interconnected transition showed areas of organized collagen alignment. After twelve weeks, parallel collagen alignment was observed in both groups that were treated with silk-fibroin scaffolds and the group in which a transversal tendon cut was conducted.

One would assume that the treatment with a collagen sponge promotes collagen formation. We were not able to confirm this assumption, as there was no apparent organisation of collagen fibers at none of the studied time points. Similar results were observed in a study by Müller et al., who tested the effect of a collagen type I sponge on Achilles tendon regeneration in rats. A trans-section of the Achilles tendon was performed in 42 rats and a collagen type I sponge was inserted into the transected area in half of the animals. Subsequently, the authors evaluated the histological properties of the regenerate. After four weeks, no difference in the collagen arrangement for the groups treated with or without the collagen sponge was found (Muller et al., 2016).

It has been reported that during intrinsic tendon healing, collagen fibers from the injured tendon are released and then reused for regeneration (Ehrlich, Lambert, Saggars, Myers, & Hauck, 2005). According to our results, it remains unassured if collagen inserted at the injury side can be recycled and integrated directly.

Teuschl et al. tested a degradable silk fiber-based scaffold for ACL reconstruction in sheep and found longitudinal alignment of collagen fibers in all regions after twelve months (Teuschl et al., 2016). Thus, silk-fibroin scaffolds seem to promote the formation of aligned collagen. As there were longitudinally orientated and organized collagen fibers found in both silk-fibroin scaffold groups, our results confirm this assumption. However, the scaffold structure seems to have an influence on time and amount of collagen formation. Since we found parallel collagen fibrils at both time points in the scaffold with the interconnected transition and only at the second time point in the abrupt transition group. This confirms the third

hypothesis that the different structures influence the regain of histopathological properties similar to the native enthesis.

5.6. LIMITATIONS AND OUTLOOK

One limitation of our study is the low sample number used. This can explain the high dispersion of values obtained during μ CT analysis, in which only a few significant differences could be obtained. Future studies with larger sample sizes and extended observation periods may confirm our initial findings.

Additionally, even though efforts were made to section all histological in the same manner, one can never accomplish an exact conformity of sections. Thereby, a little variation between the sections needs to be taken into account when assessing the histopathological findings.

The regain of mechanical properties is of great importance during enthesis regeneration (Fan et al., 2009). In our study, the samples were only examined in terms of histopathological characteristics and the occurrence of ectopic bone formation. Although one can presume that the regain of histopathological properties similar to the native enthesis correlates with the regain of resistance to mechanical stress, biomechanical testing would be necessary to verify this assumption. However, the assessment period of three months is too short to deliver final results. In further tests and after a longer observation period, the scaffold with an interconnected transition might prove a satisfying resistance to mechanical load and continuing enhancement of the enthesis regeneration. Furthermore, it was shown that immobilization during the healing period of a surgically detached and sutured supraspinatus enthesis can lead to a regain of superior structural and compositional properties (Thomopoulos et al., 2003). In this study, no differences in the loading conditions were performed but should be considered in further investigations.

Moreover, stem cells have shown good results in enhancing tissue regeneration (Bianco et al., 2019; Fan et al., 2009; Godwin, Young, Dudhia, Beamish, & Smith, 2012; Hernigou et al., 2014; Kokubu et al., 2020). The *in vivo* test of these biphasic silk-fibroin scaffolds seeded with stem cells may be interesting to further investigate.

5.7. RECAPITULATION AND CONCLUSION

The aim of this study was to examine two biphasic silk-fibroin scaffolds for enthesis regeneration in a rat model. Due to its characteristics as biocompatible and slowly degradable material, silk has been extensively tested as a biomaterial for tissue engineering applications (Altman et al., 2002; Altman et al., 2008; J. A. Cooper, Jr. et al., 2007). Furthermore, a scaffold design that incorporated different zones mimicking the natural enthesis is essential (H. H. Lu & Spalazzi, 2009).

Four hypotheses were phrased at the start of this study.

Firstly: "The implantation of silk-fibroin scaffolds into an enthesis defect leads to less ossification in the tendon compared to the control groups." The group treated with the silk-fibroin scaffold with an interconnected transition showed a lower tendency for ectopic bone formation compared to the other experimental groups. However, no significant differences between the experimental groups were found. Moreover, the silk-fibroin scaffold with the abrupt transition showed comparably high levels of ectopic bone formation after 12 weeks. Hence, the first hypothesis could not be confirmed.

Secondly: "The implantation of silk-fibroin scaffolds into an enthesis defect leads to interface healing with histological properties similar to a native enthesis." Cell density and vascularity in the groups treated with silk-fibroin scaffolds were higher than in the native enthesis. Cell alignment and collagen alignment were not as organized in the scaffold groups compared to the native enthesis. Anyhow, the interconnected transition group showed promising results in terms of supporting the natural healing capacities. The regain of histopathological characteristics similar to a native enthesis might take a longer healing period than the observation period of twelve weeks.

Thirdly: "The different structures of the silk-fibroin scaffold have an influence on the occurrence of ossification during healing and the regain of the histological characteristics of a native enthesis." This hypothesis can be considered confirmed as the scaffold with an interconnected transition showed a lower tendency to heterotopic ossification and an earlier alignment of collagen than the scaffold with an abrupt transition.

Fourthly: “Silk-fibroin is a good material for enthesis regeneration.” Two biphasic silk-fibroin scaffolds were tested in a rat model. Both showed promising results in regaining histopathological properties. Especially, the scaffold with the interconnected transition has turned out to support the natural healing capacity superiorly to the silk-fibroin scaffold with the abrupt transition. The design of the interconnected transition is simulating the structure of a natural enthesis and our results indicate that this special design supports the regain of a native enthesis structure. These results are in line with the results reported by Font Tellado et al., who have identified scaffold with the smooth transition as a promising candidate for enthesis regeneration (Font Tellado et al., 2017).

In summary, silk-fibroin scaffolds have shown promising results regarding the prevention of ectopic bone formation and the regain of histopathological properties during enthesis regeneration. The findings of this study can support the further development of scaffolds for the tendon-to-bone interface regeneration.

6. REFERENCES

- Ahmed, I. M., Lagopoulos, M., McConnell, P., Soames, R. W., & Sefton, G. K. (1998). Blood supply of the Achilles tendon. *J Orthop Res*, *16*(5), 591-596. doi:10.1002/jor.1100160511
- Altman, G. H., Horan, R. L., Lu, H. H., Moreau, J., Martin, I., Richmond, J. C., & Kaplan, D. L. (2002). Silk matrix for tissue engineered anterior cruciate ligaments. *Biomaterials*, *23*(20), 4131-4141. doi:10.1016/s0142-9612(02)00156-4
- Altman, G. H., Horan, R. L., Weitzel, P., & Richmond, J. C. (2008). The use of long-term bioresorbable scaffolds for anterior cruciate ligament repair. *J Am Acad Orthop Surg*, *16*(4), 177-187. doi:10.5435/00124635-200804000-00001
- Apostolakos, J., Durant, T. J., Dwyer, C. R., Russell, R. P., Weinreb, J. H., Alaei, F., . . . Mazzocca, A. D. (2014). The enthesis: a review of the tendon-to-bone insertion. *Muscles Ligaments Tendons J*, *4*(3), 333-342.
- Awad, H. A., Butler, D. L., Boivin, G. P., Smith, F. N., Malaviya, P., Huibregtse, B., & Caplan, A. I. (1999). Autologous mesenchymal stem cell-mediated repair of tendon. *Tissue Eng*, *5*(3), 267-277. doi:10.1089/ten.1999.5.267
- Beaulieu, M. L., Carey, G. E., Schlecht, S. H., Wojtys, E. M., & Ashton-Miller, J. A. (2015). Quantitative comparison of the microscopic anatomy of the human ACL femoral and tibial entheses. *J Orthop Res*, *33*(12), 1811-1817. doi:10.1002/jor.22966
- Benazzo, F., Zanon, G., & Maffulli, N. (2000). An Operative Approach to Achilles Tendinopathy. *Sports Medicine and Arthroscopy Review*, *8*. doi:10.1097/00132585-200008010-00009
- Benjamin, M., Kaiser, E., & Milz, S. (2008). Structure-function relationships in tendons: a review. *J Anat*, *212*(3), 211-228. doi:10.1111/j.1469-7580.2008.00864.x
- Benjamin, M., Kumai, T., Milz, S., Boszczyk, B., Boszczyk, A. A., & Ralphs, J. (2003). The Skeletal Attachment of Tendons – Tendon ‘entheses’. *Comparative biochemistry and physiology. Part A, Molecular & integrative physiology*, *133*, 931-945. doi:10.1016/S1095-6433(02)00138-1
- Benjamin, M., Moriggl, B., Brenner, E., Emery, P., McGonagle, D., & Redman, S. (2004). The "enthesis organ" concept: why enthesopathies may not present as focal insertional disorders. *Arthritis Rheum*, *50*(10), 3306-3313. doi:10.1002/art.20566
- Benjamin, M., Toumi, H., Ralphs, J. R., Bydder, G., Best, T. M., & Milz, S. (2006). Where tendons and ligaments meet bone: attachment sites ('entheses') in relation to exercise and/or mechanical load. *J Anat*, *208*(4), 471-490. doi:10.1111/j.1469-7580.2006.00540.x
- Bi, F., Shi, Z., Liu, A., Guo, P., & Yan, S. (2015). Anterior cruciate ligament reconstruction in a rabbit model using silk-collagen scaffold and comparison with autograft. *PLoS One*, *10*(5), e0125900. doi:10.1371/journal.pone.0125900
- Bianco, S. T., Moser, H. L., Galatz, L. M., & Huang, A. H. (2019). Biologics and stem cell-based therapies for rotator cuff repair. *Ann N Y Acad Sci*, *1442*(1), 35-47. doi:10.1111/nyas.13918
- Bidder, M., Towler, D. A., Gelberman, R. H., & Boyer, M. I. (2000). Expression of mRNA for vascular endothelial growth factor at the repair site of healing canine flexor tendon. *J Orthop Res*, *18*(2), 247-252. doi:10.1002/jor.1100180212
- Board, T. N., Karva, A., Board, R. E., Gambhir, A. K., & Porter, M. L. (2007). The prophylaxis and treatment of heterotopic ossification following lower limb

- arthroplasty. *J Bone Joint Surg Br*, 89(4), 434-440. doi:10.1302/0301-620X.89B4.18845
- Bosch, U., & Kasperczyk, W. J. (1992). Healing of the patellar tendon autograft after posterior cruciate ligament reconstruction--a process of ligamentization? An experimental study in a sheep model. *Am J Sports Med*, 20(5), 558-566. doi:10.1177/036354659202000513
- Burkhart, S. S., Johnson, T. C., Wirth, M. A., & Athanasiou, K. A. (1997). Cyclic loading of transosseous rotator cuff repairs: tension overload as a possible cause of failure. *Arthroscopy*, 13(2), 172-176. doi:10.1016/s0749-8063(97)90151-1
- Butler, D. L., Juncosa-Melvin, N., Boivin, G. P., Galloway, M. T., Shearn, J. T., Gooch, C., & Awad, H. (2008). Functional tissue engineering for tendon repair: A multidisciplinary strategy using mesenchymal stem cells, bioscaffolds, and mechanical stimulation. *J Orthop Res*, 26(1), 1-9. doi:10.1002/jor.20456
- Cai, L., Wang, Z., Luo, X., She, W., & Zhang, H. (2019). Optimal strategies for the prevention of heterotopic ossification after total hip arthroplasty: A network meta-analysis. *Int J Surg*, 62, 74-85. doi:10.1016/j.ijssu.2018.12.011
- Calejo, I., Costa-Almeida, R., Reis, R. L., & Gomes, M. E. (2019). Enthesis Tissue Engineering: Biological Requirements Meet at the Interface. *Tissue Eng Part B Rev*, 25(4), 330-356. doi:10.1089/ten.TEB.2018.0383
- Cao, Y., & Wang, B. (2009). Biodegradation of silk biomaterials. *Int J Mol Sci*, 10(4), 1514-1524. doi:10.3390/ijms10041514
- Carr, A. J., & Norris, S. H. (1989). The blood supply of the calcaneal tendon. *J Bone Joint Surg Br*, 71(1), 100-101. doi:10.1302/0301-620x.71b1.2914976
- Chang, J., Most, D., Thunder, R., Mehrara, B., Longaker, M. T., & Lineaweaver, W. C. (1998). Molecular studies in flexor tendon wound healing: the role of basic fibroblast growth factor gene expression. *J Hand Surg Am*, 23(6), 1052-1058. doi:10.1016/S0363-5023(98)80015-4
- Cooper, J. A., Jr., Sahota, J. S., Gorum, W. J., 2nd, Carter, J., Doty, S. B., & Laurencin, C. T. (2007). Biomimetic tissue-engineered anterior cruciate ligament replacement. *Proc Natl Acad Sci U S A*, 104(9), 3049-3054. doi:10.1073/pnas.0608837104
- Cooper, J. A., Lu, H. H., Ko, F. K., Freeman, J. W., & Laurencin, C. T. (2005). Fiber-based tissue-engineered scaffold for ligament replacement: design considerations and in vitro evaluation. *Biomaterials*, 26(13), 1523-1532. doi:10.1016/j.biomaterials.2004.05.014
- Craven, P. L., & Urist, M. R. (1971). Osteogenesis by radioisotope labelled cell populations in implants of bone matrix under the influence of ionizing radiation. *Clin Orthop Relat Res*, 76, 231-243. doi:10.1097/00003086-197105000-00030
- Davis, T. A., O'Brien, F. P., Anam, K., Grijalva, S., Potter, B. K., & Elster, E. A. (2011). Heterotopic ossification in complex orthopaedic combat wounds: quantification and characterization of osteogenic precursor cell activity in traumatized muscle. *J Bone Joint Surg Am*, 93(12), 1122-1131. doi:10.2106/JBJS.J.01417
- Dean, B. J., Franklin, S. L., & Carr, A. J. (2012). A systematic review of the histological and molecular changes in rotator cuff disease. *Bone Joint Res*, 1(7), 158-166. doi:10.1302/2046-3758.17.2000115
- Docheva, D., Muller, S. A., Majewski, M., & Evans, C. H. (2015). Biologics for tendon repair. *Adv Drug Deliv Rev*, 84, 222-239. doi:10.1016/j.addr.2014.11.015
- Duffy, F. J., Jr., Seiler, J. G., Gelberman, R. H., & Hergrueter, C. A. (1995). Growth factors and canine flexor tendon healing: initial studies in uninjured and repair models. *J Hand Surg Am*, 20(4), 645-649. doi:10.1016/S0363-5023(05)80284-9

- Ehrlich, H. P., Lambert, P. A., Siggers, G. C., Myers, R. L., & Hauck, R. M. (2005). Dynamic changes appearing in collagen fibers during intrinsic tendon repair. *Ann Plast Surg*, *54*(2), 201-206. doi:10.1097/01.sap.0000141380.52782.db
- Evans, E. J., Benjamin, M., & Pemberton, D. J. (1990). Fibrocartilage in the attachment zones of the quadriceps tendon and patellar ligament of man. *J Anat*, *171*, 155-162.
- Fan, H., Liu, H., Toh, S. L., & Goh, J. C. (2009). Anterior cruciate ligament regeneration using mesenchymal stem cells and silk scaffold in large animal model. *Biomaterials*, *30*(28), 4967-4977. doi:10.1016/j.biomaterials.2009.05.048
- Fenwick, S. A., Hazleman, B. L., & Riley, G. P. (2002). The vasculature and its role in the damaged and healing tendon. *Arthritis Res*, *4*(4), 252-260. doi:10.1186/ar416
- Font Tellado, S., Balmayor, E. R., & Van Griensven, M. (2015). Strategies to engineer tendon/ligament-to-bone interface: Biomaterials, cells and growth factors. *Adv Drug Deliv Rev*, *94*, 126-140. doi:10.1016/j.addr.2015.03.004
- Font Tellado, S., Bonani, W., Balmayor, E. R., Foehr, P., Motta, A., Migliaresi, C., & van Griensven, M. (2017). (*) Fabrication and Characterization of Biphasic Silk Fibroin Scaffolds for Tendon/Ligament-to-Bone Tissue Engineering. *Tissue Eng Part A*, *23*(15-16), 859-872. doi:10.1089/ten.TEA.2016.0460
- Font Tellado, S., Chiera, S., Bonani, W., Poh, P. S. P., Migliaresi, C., Motta, A., . . . van Griensven, M. (2018). Heparin functionalization increases retention of TGF-beta2 and GDF5 on biphasic silk fibroin scaffolds for tendon/ligament-to-bone tissue engineering. *Acta Biomater*, *72*, 150-166. doi:10.1016/j.actbio.2018.03.017
- Franchi, M., Trire, A., Quaranta, M., Orsini, E., & Ottani, V. (2007). Collagen structure of tendon relates to function. *ScientificWorldJournal*, *7*, 404-420. doi:10.1100/tsw.2007.92
- Galatz, L. M., Ball, C. M., Teefey, S. A., Middleton, W. D., & Yamaguchi, K. (2004). The outcome and repair integrity of completely arthroscopically repaired large and massive rotator cuff tears. *J Bone Joint Surg Am*, *86*(2), 219-224. doi:10.2106/00004623-200402000-00002
- Galatz, L. M., Rothermich, S. Y., Zaegel, M., Silva, M. J., Havlioglu, N., & Thomopoulos, S. (2005). Delayed repair of tendon to bone injuries leads to decreased biomechanical properties and bone loss. *J Orthop Res*, *23*(6), 1441-1447. doi:10.1016/j.orthres.2005.05.005.1100230629
- Gaspar, D., Spanoudes, K., Holladay, C., Pandit, A., & Zeugolis, D. (2015). Progress in cell-based therapies for tendon repair. *Adv Drug Deliv Rev*, *84*, 240-256. doi:10.1016/j.addr.2014.11.023
- Gelberman, R. H. (1985). Flexor tendon physiology: tendon nutrition and cellular activity in injury and repair. *Instr Course Lect*, *34*, 351-360.
- Godwin, E. E., Young, N. J., Dudhia, J., Beamish, I. C., & Smith, R. K. (2012). Implantation of bone marrow-derived mesenchymal stem cells demonstrates improved outcome in horses with overstrain injury of the superficial digital flexor tendon. *Equine Vet J*, *44*(1), 25-32. doi:10.1111/j.2042-3306.2011.00363.x
- Hernigou, P., Flouzat Lachaniette, C. H., Delambre, J., Zilber, S., Duffiet, P., Chevallier, N., & Rouard, H. (2014). Biologic augmentation of rotator cuff repair with mesenchymal stem cells during arthroscopy improves healing and prevents further tears: a case-controlled study. *Int Orthop*, *38*(9), 1811-1818. doi:10.1007/s00264-014-2391-1
- Hoffmann, A., & Gross, G. (2006). Tendon and ligament engineering: from cell biology to in vivo application. *Regen Med*, *1*(4), 563-574. doi:10.2217/17460751.1.4.563

- Hope, M., & Saxby, T. S. (2007). Tendon healing. *Foot Ankle Clin*, 12(4), 553-567, v. doi:10.1016/j.fcl.2007.07.003
- Hurlimann, M., Schiapparelli, F. F., Rotigliano, N., Testa, E., Amsler, F., & Hirschmann, M. T. (2017). Influence of surgical approach on heterotopic ossification after total hip arthroplasty - is minimal invasive better? A case control study. *BMC Musculoskelet Disord*, 18(1), 27. doi:10.1186/s12891-017-1391-x
- Hyman, J., & Rodeo, S. A. (2000). Injury and repair of tendons and ligaments. *Phys Med Rehabil Clin N Am*, 11(2), 267-288, v.
- Jain, N. B., Higgins, L. D., Losina, E., Collins, J., Blazar, P. E., & Katz, J. N. (2014). Epidemiology of musculoskeletal upper extremity ambulatory surgery in the United States. *BMC Musculoskelet Disord*, 15, 4. doi:10.1186/1471-2474-15-4
- James, R., Kesturu, G., Balian, G., & Chhabra, A. B. (2008). Tendon: biology, biomechanics, repair, growth factors, and evolving treatment options. *J Hand Surg Am*, 33(1), 102-112. doi:10.1016/j.jhsa.2007.09.007
- Kaeding, C. C., Aros, B., Pedroza, A., Pifel, E., Amendola, A., Andrish, J. T., . . . Spindler, K. P. (2011). Allograft Versus Autograft Anterior Cruciate Ligament Reconstruction: Predictors of Failure From a MOON Prospective Longitudinal Cohort. *Sports Health*, 3(1), 73-81. doi:10.1177/1941738110386185
- Kannus, P. (2000). Structure of the tendon connective tissue. *Scand J Med Sci Sports*, 10(6), 312-320. doi:10.1034/j.1600-0838.2000.010006312.x
- Kannus, P., & Jozsa, L. (1991). Histopathological changes preceding spontaneous rupture of a tendon. A controlled study of 891 patients. *J Bone Joint Surg Am*, 73(10), 1507-1525.
- Kasperczyk, W. J., Bosch, U., Oestern, H. J., & Tscherne, H. (1993). Staging of patellar tendon autograft healing after posterior cruciate ligament reconstruction. A biomechanical and histological study in a sheep model. *Clin Orthop Relat Res*(286), 271-282.
- Khan, K. M., Cook, J. L., Bonar, F., Harcourt, P., & Astrom, M. (1999). Histopathology of common tendinopathies. Update and implications for clinical management. *Sports Med*, 27(6), 393-408. doi:10.2165/00007256-199927060-00004
- Kirkendall, D. T., & Garrett, W. E. (1997). Function and biomechanics of tendons. *Scand J Med Sci Sports*, 7(2), 62-66. doi:10.1111/j.1600-0838.1997.tb00120.x
- Kokubu, S., Inaki, R., Hoshi, K., & Hikita, A. (2020). Adipose-derived stem cells improve tendon repair and prevent ectopic ossification in tendinopathy by inhibiting inflammation and inducing neovascularization in the early stage of tendon healing. *Regen Ther*, 14, 103-110. doi:10.1016/j.reth.2019.12.003
- Kuroda, R., Kurosaka, M., Yoshiya, S., & Mizuno, K. (2000). Localization of growth factors in the reconstructed anterior cruciate ligament: immunohistological study in dogs. *Knee Surg Sports Traumatol Arthrosc*, 8(2), 120-126. doi:10.1007/s001670050198
- Langer, R., & Vacanti, J. P. (1993). Tissue engineering. *Science*, 260(5110), 920-926. doi:10.1126/science.8493529
- Li, H., Fan, J., Sun, L., Liu, X., Cheng, P., & Fan, H. (2016). Functional regeneration of ligament-bone interface using a triphasic silk-based graft. *Biomaterials*, 106, 180-192. doi:10.1016/j.biomaterials.2016.08.012
- Lim, W. L., Liao, L. L., Ng, M. H., Chowdhury, S. R., & Law, J. X. (2019). Current Progress in Tendon and Ligament Tissue Engineering. *Tissue Engineering and Regenerative Medicine*, 16(6), 549-571. doi:10.1007/s13770-019-00196-w
- Lin, T. W., Cardenas, L., & Soslowky, L. J. (2004). Biomechanics of tendon injury and repair. *J Biomech*, 37(6), 865-877. doi:10.1016/j.jbiomech.2003.11.005

- Lipman, K., Wang, C., Ting, K., Soo, C., & Zheng, Z. (2018). Tendinopathy: injury, repair, and current exploration. *Drug design, development and therapy*, *12*, 591-603. doi:10.2147/DDDT.S154660
- Lomas, A. J., Ryan, C. N., Sorushanova, A., Shologu, N., Sideri, A. I., Tsioli, V., . . . Zeugolis, D. I. (2015). The past, present and future in scaffold-based tendon treatments. *Adv Drug Deliv Rev*, *84*, 257-277. doi:10.1016/j.addr.2014.11.022
- Loppini, M., Longo, U. G., Niccoli, G., Khan, W. S., Maffulli, N., & Denaro, V. (2015). Histopathological scores for tissue-engineered, repaired and degenerated tendon: a systematic review of the literature. *Curr Stem Cell Res Ther*, *10*(1), 43-55. doi:10.2174/1574888x09666140710110723
- Lu, D., Yang, C., Zhang, Z., & Xiao, M. (2018). Enhanced tendon-bone healing with acidic fibroblast growth factor delivered in collagen in a rabbit anterior cruciate ligament reconstruction model. *J Orthop Surg Res*, *13*(1), 301. doi:10.1186/s13018-018-0984-x
- Lu, H. H., & Spalazzi, J. P. (2009). Biomimetic stratified scaffold design for ligament-to-bone interface tissue engineering. *Comb Chem High Throughput Screen*, *12*(6), 589-597. doi:10.2174/138620709788681925
- Lu, H. H., & Thomopoulos, S. (2013). Functional attachment of soft tissues to bone: development, healing, and tissue engineering. *Annu Rev Biomed Eng*, *15*, 201-226. doi:10.1146/annurev-bioeng-071910-124656
- McFarland, E. G., Morrey, B. F., An, K. N., & Wood, M. B. (1986). The relationship of vascularity and water content to tensile strength in a patellar tendon replacement of the anterior cruciate in dogs. *Am J Sports Med*, *14*(6), 436-448. doi:10.1177/036354658601400602
- Mitchell, A. C., Briquez, P. S., Hubbell, J. A., & Cochran, J. R. (2016). Engineering growth factors for regenerative medicine applications. *Acta Biomater*, *30*, 1-12. doi:10.1016/j.actbio.2015.11.007
- Moffat, K. L., Sun, W. H., Pena, P. E., Chahine, N. O., Doty, S. B., Ateshian, G. A., . . . Lu, H. H. (2008). Characterization of the structure-function relationship at the ligament-to-bone interface. *Proc Natl Acad Sci U S A*, *105*(23), 7947-7952. doi:10.1073/pnas.0712150105
- Moshiri, A., & Oryan, A. (2012). Role of tissue engineering in tendon reconstructive surgery and regenerative medicine: Current concepts, approaches and concerns. *Hard Tissue*, *1*, 11. doi:10.13172/2050-2303-1-2-291
- Moshiri, A., & Oryan, A. (2013). tendon-and-ligament-tissue-engineering-healing-and-regenerative-medicine-2161-0673.1000126. *Journal of Sports Medicine & Doping Studies*, *3*, 126. doi:10.4172/2161-0673.1000126
- Moshiri, A., Oryan, A., & Meimandi-Parizi, A. (2013). Role of tissue-engineered artificial tendon in healing of a large Achilles tendon defect model in rabbits. *J Am Coll Surg*, *217*(3), 421-441.e428. doi:10.1016/j.jamcollsurg.2013.03.025
- Mueller, M. (2011). *Chirurgie (2012/13)* (Vol. 11): Medizinische Verlags- und Informationsdienste.
- Muller, S. A., Durselen, L., Heisterbach, P., Evans, C., & Majewski, M. (2016). Effect of a Simple Collagen Type I Sponge for Achilles Tendon Repair in a Rat Model. *Am J Sports Med*, *44*(8), 1998-2004. doi:10.1177/0363546516641942
- Mullisch, M., & Welsch, U. (2010). *Romeis - Mikroskopische Technik* (Vol. 18): Spektrum Akademischer Verlag.
- Nikolaou, P. K., Seaber, A. V., Glisson, R. R., Ribbeck, B. M., & Bassett, F. H., 3rd. (1986). Anterior cruciate ligament allograft transplantation. Long-term function,

- histology, revascularization, and operative technique. *Am J Sports Med*, 14(5), 348-360. doi:10.1177/036354658601400502
- Nourissat, G., Berenbaum, F., & Duprez, D. (2015). Tendon injury: from biology to tendon repair. *Nat Rev Rheumatol*, 11(4), 223-233. doi:10.1038/nrrheum.2015.26
- O'Brien, M. (2005). Anatomy of Tendons. In N. Maffulli, P. Renström, & W. B. Leadbetter (Eds.), *Tendon Injuries: Basic Science and Clinical Medicine* (pp. 3-13). London: Springer London.
- Peniche Silva, C. J., Müller, S. A., Quirk, N., Poh, P. S. P., Mayer, C., Motta, A., . . . van Griensven, M. (2022). Enthesis Healing Is Dependent on Scaffold Interphase Morphology-Results from a Rodent Patellar Model. *Cells*, 11(11). doi:10.3390/cells11111752
- Qian, S., Wang, Z., Zheng, Z., Ran, J., Zhu, J., & Chen, W. (2019). A Collagen and Silk Scaffold for Improved Healing of the Tendon and Bone Interface in a Rabbit Model. *Med Sci Monit*, 25, 269-278. doi:10.12659/MSM.912038
- Qu, D., Mosher, C. Z., Boushell, M. K., & Lu, H. H. (2015). Engineering complex orthopaedic tissues via strategic biomimicry. *Ann Biomed Eng*, 43(3), 697-717. doi:10.1007/s10439-014-1190-6
- Rawson, S., Cartmell, S., & Wong, J. (2013). Suture techniques for tendon repair; a comparative review. *Muscles Ligaments Tendons J*, 3(3), 220-228.
- Riley, G. (2004). The pathogenesis of tendinopathy. A molecular perspective. *Rheumatology (Oxford)*, 43(2), 131-142. doi:10.1093/rheumatology/keg448
- Rittié, L. (2017). Method for Picrosirius Red-Polarization Detection of Collagen Fibers in Tissue Sections. *Methods Mol Biol*, 1627, 395-407. doi:10.1007/978-1-4939-7113-8_26
- Sahoo, S., Teh, T., He, P., Toh, S. L., & Goh, J. (2011). Interface tissue engineering: next phase in musculoskeletal tissue repair. *Ann Acad Med Singap*, 40(5), 245-251.
- Santo, V. E., Gomes, M. E., Mano, J. F., & Reis, R. L. (2013). Controlled release strategies for bone, cartilage, and osteochondral engineering--Part II: challenges on the evolution from single to multiple bioactive factor delivery. *Tissue Eng Part B Rev*, 19(4), 327-352. doi:10.1089/ten.TEB.2012.0727
- Schmidt-Rohlfing, B., Graf, J., Schneider, U., & Niethard, F. U. (1992). The blood supply of the Achilles tendon. *Int Orthop*, 16(1), 29-31. doi:10.1007/BF00182980
- Schmitz, N., Laverty, S., Kraus, V. B., & Aigner, T. (2010). Basic methods in histopathology of joint tissues. *Osteoarthritis Cartilage*, 18 Suppl 3, S113-116. doi:10.1016/j.joca.2010.05.026
- Schneider, M., Angele, P., Jarvinen, T. A. H., & Docheva, D. (2018). Rescue plan for Achilles: Therapeutics steering the fate and functions of stem cells in tendon wound healing. *Adv Drug Deliv Rev*, 129, 352-375. doi:10.1016/j.addr.2017.12.016
- Selvanetti, A., Cipolla, M., & Puddu, G. (1997). Overuse tendon injuries: Basic science and classification. *Operative Techniques in Sports Medicine*, 5(3), 110-117. doi:10.1016/S1060-1872(97)80031-7
- Sharma, P., & Maffulli, N. (2005). Basic biology of tendon injury and healing. *The surgeon : journal of the Royal Colleges of Surgeons of Edinburgh and Ireland*, 3, 309-316. doi:10.1016/S1479-666X(05)80109-X
- Sharma, P., & Maffulli, N. (2006). Biology of tendon injury: healing, modeling and remodeling. *J Musculoskelet Neuronal Interact*, 6(2), 181-190.
- Shaw, H. M., & Benjamin, M. (2007). Structure-function relationships of entheses in relation to mechanical load and exercise. *Scand J Med Sci Sports*, 17(4), 303-315. doi:10.1111/j.1600-0838.2007.00689.x

- Shelton, W. R., & Fagan, B. C. (2011). Autografts commonly used in anterior cruciate ligament reconstruction. *J Am Acad Orthop Surg*, 19(5), 259-264. doi:10.5435/00124635-201105000-00003
- Shen, W., Chen, J., Yin, Z., Chen, X., Liu, H., Heng, B. C., . . . Ouyang, H. W. (2012). Allogeneous tendon stem/progenitor cells in silk scaffold for functional shoulder repair. *Cell Transplant*, 21(5), 943-958. doi:10.3727/096368911x627453
- Silva, C., Carretero, A., Soares da Costa, D., Reis, R. L., Novoa-Carballal, R., & Pashkuleva, I. (2017). Design of protein delivery systems by mimicking extracellular mechanisms for protection of growth factors. *Acta Biomater*, 63, 283-293. doi:10.1016/j.actbio.2017.08.042
- Smietana, M. J., Moncada-Larrotiz, P., Arruda, E. M., Bedi, A., & Larkin, L. M. (2017). Tissue-Engineered Tendon for Enthesis Regeneration in a Rat Rotator Cuff Model. *Biores Open Access*, 6(1), 47-57. doi:10.1089/biores.2016.0042
- Smith, L., Xia, Y., Galatz, L. M., Genin, G. M., & Thomopoulos, S. (2012). Tissue-engineering strategies for the tendon/ligament-to-bone insertion. *Connect Tissue Res*, 53(2), 95-105. doi:10.3109/03008207.2011.650804
- Snedeker, J. G., & Foolen, J. (2017). Tendon injury and repair - A perspective on the basic mechanisms of tendon disease and future clinical therapy. *Acta Biomater*, 63, 18-36. doi:10.1016/j.actbio.2017.08.032
- Tadros, A. S., Huang, B. K., & Pathria, M. N. (2018). Muscle-Tendon-Enthesis Unit. *Semin Musculoskelet Radiol*, 22(3), 263-274. doi:10.1055/s-0038-1641570
- Taylor, D. C., Dalton, J. D., Jr., Seaber, A. V., & Garrett, W. E., Jr. (1993). Experimental muscle strain injury. Early functional and structural deficits and the increased risk for reinjury. *Am J Sports Med*, 21(2), 190-194. doi:10.1177/036354659302100205
- Tellado, S. F. (2018). *Tissue engineering of the tendon/ligament-to-bone transition*. (Dissertation zur Erlangung des akademischen Grades eines Doktor der Naturwissenschaften (Dr. rer. nat.)). Technische Universität München, München.
- Teuschl, A., Heimel, P., Nurnberger, S., van Griensven, M., Redl, H., & Nau, T. (2016). A Novel Silk Fiber-Based Scaffold for Regeneration of the Anterior Cruciate Ligament: Histological Results From a Study in Sheep. *Am J Sports Med*, 44(6), 1547-1557. doi:10.1177/0363546516631954
- Thomopoulos, S., Genin, G. M., & Galatz, L. M. (2010). The development and morphogenesis of the tendon-to-bone insertion - what development can teach us about healing. *J Musculoskelet Neuronal Interact*, 10(1), 35-45.
- Thomopoulos, S., Williams, G. R., & Soslowsky, L. J. (2003). Tendon to bone healing: differences in biomechanical, structural, and compositional properties due to a range of activity levels. *J Biomech Eng*, 125(1), 106-113. doi:10.1115/1.1536660
- Thorpe, C. T., & Screen, H. R. C. (2016). Tendon Structure and Composition. In P. W. Ackermann & D. A. Hart (Eds.), *Metabolic Influences on Risk for Tendon Disorders* (pp. 3-10). Cham: Springer International Publishing.
- Voleti, P. B., Buckley, M. R., & Soslowsky, L. J. (2012). Tendon healing: repair and regeneration. *Annu Rev Biomed Eng*, 14, 47-71. doi:10.1146/annurev-bioeng-071811-150122
- Walden, G., Liao, X., Donell, S., Raxworthy, M. J., Riley, G. P., & Saeed, A. (2017). A Clinical, Biological, and Biomaterials Perspective into Tendon Injuries and Regeneration. *Tissue Eng Part B Rev*, 23(1), 44-58. doi:10.1089/ten.TEB.2016.0181
- Wang, J. H. (2006). Mechanobiology of tendon. *J Biomech*, 39(9), 1563-1582. doi:10.1016/j.jbiomech.2005.05.011

- Watkins, J. P., Auer, J. A., Morgan, S. J., & Gay, S. (1985). Healing of surgically created defects in the equine superficial digital flexor tendon: effects of pulsing electromagnetic field therapy on collagen-type transformation and tissue morphologic reorganization. *Am J Vet Res*, *46*(10), 2097-2103.
- Wu, F., Nerlich, M., & Docheva, D. (2017). Tendon injuries: Basic science and new repair proposals. *EFORT Open Rev*, *2*(7), 332-342. doi:10.1302/2058-5241.2.160075
- Xu, R., Hu, J., Zhou, X., & Yang, Y. (2018). Heterotopic ossification: Mechanistic insights and clinical challenges. *Bone*, *109*, 134-142. doi:10.1016/j.bone.2017.08.025
- Young, R. G., Butler, D. L., Weber, W., Caplan, A. I., Gordon, S. L., & Fink, D. J. (1998). Use of mesenchymal stem cells in a collagen matrix for Achilles tendon repair. *J Orthop Res*, *16*(4), 406-413. doi:10.1002/jor.1100160403
- Zafar, M. S., Mahmood, A., & Maffulli, N. (2009). Basic Science and Clinical Aspects of Achilles Tendinopathy. *Sports Medicine and Arthroscopy Review*, *17*(3), 190-197. doi:10.1097/JSA.0b013e3181b37eb7
- Zhang, Q., Zhou, D., Wang, H., & Tan, J. (2020). Heterotopic ossification of tendon and ligament. *J Cell Mol Med*, *24*(10), 5428-5437. doi:10.1111/jcmm.15240

7. APPENDIX

7.1. LIST OF FIGURES

- Fig. 1: Tendon structure.
- Fig. 2: Structure and composition of fibrocartilaginous enthesis.
- Fig. 3: Illustration of the four zones of the enthesis in a mouse supraspinatus. Staining in toluidine blue.
- Fig. 4: Stages of tendon repair. In the timeline: h = hours, M = months, and Y = years.
- Fig. 5: Structure of biphasic silk fibroin scaffolds. μ CT reconstruction (A), field emission scanning electron microscopy and fluorescent microscopy (B) illustrating the morphology of the areas with anisotropic and isotropic porosity and the transition zone. Scale bars = 300 μ m.
- Fig. 6: Selection of bone belonging to the patella and the tibia in CTAnalyser.
- Fig. 7: A ROI that was considered for the calculation of the bone mass was selected in CTAnalyser.
- Fig. 8: Micro-CT results after 4 weeks; red columns display the mean bone volume of all samples within the same group. The black vertical line shows the standard deviation.
- Fig. 9: Micro-CT results after 12 weeks; red columns display the mean bone volume of all samples within the same group. The black vertical line shows the standard deviation.
- Fig. 10: Representative images of the specimens stained with Hematoxylin and Eosin. Native enthesis in the control group is indicated by a black oval. Black arrows indicate areas with high cellularity. Red circles indicate areas with parallel cell alignment.
- Fig. 11: Representative slides for each group stained with Masson Goldner Trichrome. Black arrows indicate the presence of blood vessels.
- Fig. 12: Representative slides for each group stained with Picro-Sirius Red. White arrows indicate areas with organized collagen alignment.

7.2. LIST OF TABLES

- Table 1: Experimental groups included in the study. Applied treatment and groups are listed as well as sample numbers used for μ CT evaluation.
- Table 2: Slide number of each staining and time point.
- Table 3: Cell density in enthesis specimens harvested at 4- and 12-weeks post-surgery. Low cellularity is indicated by +, moderate cellularity by ++, and high cellularity by +++.
- Table 4: Cell alignment in tendinous part; Hardly any alignment detectable: -, alignment in few areas: +, organized alignment of tenocytes: ++.
- Table 5: Vascularity in harvested enthesis specimens: few blood vessels in enthesis are indicated by -, some blood vessels by +, and several blood vessels by ++.
- Table 6: Collagen alignment in harvested enthesis specimens: few organized areas indicated by -, several organized areas by +, and organized tendon-to-bone junction by ++.

7.3. PERMISSION TO INCLUDE PUBLISHED WORK IN THE DOCTORAL THESIS

This Agreement between Ms. Carla Mayer ("You") and Elsevier ("Elsevier") consists of your license details and the terms and conditions provided by Elsevier and Copyright Clearance Center.

License Number	5303231318702
License date	May 06, 2022
Licensed Content Publisher	Elsevier
Licensed Content Publication	Advanced Drug Delivery Reviews
Licensed Content Title	Biologics for tendon repair
Licensed Content Author	Denitsa Docheva, Sebastian A. Müller, Martin Majewski, Christopher H. Evans
Licensed Content Date	Apr 1, 2015
Licensed Content Volume	84
Licensed Content Issue	n/a
Licensed Content Pages	18
Start Page	222
End Page	239
Type of Use	reuse in a thesis/dissertation
Portion	figures/tables/illustrations
Number of figures/tables/illustrations	1
Format	both print and electronic
Are you the author of this Elsevier article?	No
Will you be translating?	No
Title	Micro-CT and Histological Evaluation of a Tissue-Engineered Enthesis in a Rat Model: Comparison to Native Tissue
Institution name	Technische Universität München
Expected presentation date	Sep 2022
Portions	Figure 1
Requestor Location	Ms. Carla Mayer Adalbertstr. 41a

This Agreement between Ms. Carla Mayer ("You") and Elsevier ("Elsevier") consists of your license details and the terms and conditions provided by Elsevier and Copyright Clearance Center.

License Number	5303220604608
License date	May 06, 2022
Licensed Content Publisher	Elsevier
Licensed Content Publication	Advanced Drug Delivery Reviews
Licensed Content Title	Strategies to engineer tendon/ligament-to-bone interface: Biomaterials, cells and growth factors
Licensed Content Author	Sonia Font Tellado,Elizabeth R. Balmayor,Martijn Van Griensven
Licensed Content Date	Nov 1, 2015
Licensed Content Volume	94
Licensed Content Issue	n/a
Licensed Content Pages	15
Start Page	126
End Page	140
Type of Use	reuse in a thesis/dissertation
Portion	figures/tables/illustrations
Number of figures/tables/illustrations	1
Format	both print and electronic
Are you the author of this Elsevier article?	No
Will you be translating?	No
Title	Micro-CT and Histological Evaluation of a Tissue-Engineered Enthesis in a Rat Model: Comparison to Native Tissue
Institution name	Technische Universität München
Expected presentation date	Sep 2022
Portions	Figure 2
Requestor Location	Ms. Carla Mayer Adalbertstr. 41a

Dear Carla Mayer,
I am from the Editorial Office of MLTJ.
You are free to use the image, but we request to cite the journal, the title of the article, the volume, the issue and the pages where the figure is published.

Thank you for your interests,

Sincerely,
Jessica Guenzi
Publishing Editor
EDRA S.p.A.
Via Spadolini 7
20141 Milan
tel. 02 8929 3926



This is a License Agreement between CARLA KONSTANZE MAYER ("User") and Copyright Clearance Center, Inc. ("CCC") on behalf of the Rightsholder identified in the order details below. The license consists of the order details, the CCC Terms and Conditions below, and any Rightsholder Terms and Conditions which are included below. All payments must be made in full to CCC in accordance with the CCC Terms and Conditions below.

Order Date	06-May-2022	Type of Use	Republish in a thesis/dissertation
Order License ID	1218887-1	Publisher	MARY ANN LIEBERT INC
ISSN	1937-335X	Portion	Image/photo/illustration

LICENSED CONTENT

Publication Title	Tissue engineering	Publication Type	e-Journal
Article Title	* Fabrication and Characterization of Biphasic Silk Fibroin Scaffolds for Tendon/Ligament-to-Bone Tissue Engineering.	Start Page	859
		End Page	872
		Issue	15-16
Date	01/01/2008	Volume	23
Language	English	URL	http://www.liebertonline.com/tea
Country	United States of America		
Rightsholder	Mary Ann Liebert Inc.		

REUSE CONTENT DETAILS

Title, description or numeric reference of the portion(s)	Figure 3	Title of the article/chapter the portion is from	* Fabrication and Characterization of Biphasic Silk Fibroin Scaffolds for Tendon/Ligament-to-Bone Tissue Engineering.
Editor of portion(s)	Font Tellado, Sònia; Bonani, Walter; Balmayor, Elizabeth R; Foehr, Peter; Motta, Antonella; Migliaresi, Claudio; van Griensven, Martijn	Author of portion(s)	Font Tellado, Sònia; Bonani, Walter; Balmayor, Elizabeth R; Foehr, Peter; Motta, Antonella; Migliaresi, Claudio; van Griensven, Martijn
Volume of serial or monograph	23		
Page or page range of portion	859-872	Issue, if republishing an article from a serial	15-16
		Publication date of portion	2017-08-01

7.4. MATERIAL LIST

Staining reagent	Producer
Direct Red 80	Sigma-Aldich Co., Missouri, USA
Eosin Y solution 0,5% in water	Carl Roth GmbH+Co. KG, Karlsruhe, Germany
Goldner-Stain I	Carl Roth GmbH+Co. KG, Karlsruhe, Germany
Goldner-Stain II	Carl Roth GmbH+Co. KG, Karlsruhe, Germany
Goldner Stain III	Carl Roth GmbH+Co. KG, Karlsruhe, Germany
Hem alum solution acid acc to Mayer	Carl Roth GmbH+Co. KG, Karlsruhe, Germany
Hematoxylin solution A acc to Weigert	Carl Roth GmbH+Co. KG, Karlsruhe, Germany
Hematoxylin solution B to Weigert	Carl Roth GmbH+Co. KG, Karlsruhe, Germany

Reagent	Producer
Acetic acid	Carl Roth GmbH+Co. KG, Karlsruhe, Germany
Aqua	B. Braun Melsungen AG, Germany
Dulbecco's Phosphate Buffer Saline	Sigma-Aldich Co., Missouri, USA
Ethanol 70%	Otto Fischar GmbH, Saarbrücken, Germany
Ethanol 100%	Otto Fischar GmbH, Saarbrücken, Germany
Ethylendiamintetraacetic acid disodium salt dihydrate	Carl Roth GmbH+Co. KG, Karlsruhe, Germany
Picrid acid solution 1,3% in water	Sigma-Aldich Co., Missouri, USA
Roti Histokitt II	Carl Roth GmbH+Co. KG, Karlsruhe, Germany

Roti-Histol	Carl Roth GmbH+Co. KG, Karlsruhe, Germany
Sodium hydroxide solution 50%	Carl Roth GmbH+Co. KG, Karlsruhe, Germany

Equipment	Producer
Adobe Illustrator 2020	Adobe Systems Software Ireland Limited, Dublin, Republic of Ireland
Adobe Lightroom	Adobe Systems Software Ireland Limited, Dublin, Republic of Ireland
Electronic balance, Kern 572	KERN & Sohn GmbH, Balingen, Germany
Electronic pipette	Eppendorf AG, Hamburg, Germany
Embedding module, Tissue-Tek	Sakura Finetek Europe B.V., Alphen aan den Rijn, Netherlands
Fluorescence microscope, BIOREVO BZ-9000	Keyence Corporation, Osaka, Japan
<i>In vivo</i> μ CT Skyscan 1176	Bruker Corporation, Billerica, USA
Magnetic stirrer	IKA-Werke GmbH & Co. KG, Staufen im Breisgau, Germany
Microsoft Office	Microsoft Corporation, Redmond, USA
Microtome Leica RM 2165	Leica Biosystems Nussloch GmbH, Nussloch, Germany
Pipette controller Accu-jet pro	BRAND GmbH & Co. KG, Wertheim, Germany
Pipet controller, Stripettor Plus	Corning Incorporated, Corning, USA
pH-Meter PB-11	Sartorius AG, Göttingen, Germany
Refrigerator 4°C	Robert Bosch GmbH, Stuttgart, Germany Liebherr International-Deutschland GmbH, Biberach an der Riß, Germany

Tissue Processor Excelsior	Thermo Fisher Scientific Inc., Waltham, USA
Vortex Genie 2	Scientific Industries Inc., Bohemia, USA
Water bath HI 1210	Leica Biosystems Nussloch GmbH, Nussloch, Germany
Polarized light microscope Olympus IX 83	Olympus Corporation of the Americas, Westborough, USA

Material	Producer
Cover slips 24x60mm	Carl Roth GmbH+Co. KG, Karlsruhe, Germany
Medical examination gloves, Size M	ABENA GmbH, Oberderdingen, Germany
Microscope Slides, Menzel-Gläser, Superfrost Plus	Thermo Fisher Scientific Inc., Waltham, USA
Microslide box	VWR International bvba, Leuven, Belgium
Microtome blades S35	pfm medical ag, Köln, Germany
Pasteur pipettes	Carl Roth GmbH+Co. KG, Karlsruhe, Germany
Pipette tips, TipOne filter tips	STARLAB International GmbH, Hamburg, Germany
Serological pipette (5ml, 10ml, 25ml, 50ml)	Greiner Bio-One International GmbH, Kremsmünster, Austria
Tube 15 ml	SARSTEDT Aktiengesellschaft & Co., Nümbrecht, Germany

8. ACKNOWLEDGMENTS

I want to thank my supervisor, Univ.-Prof. Dr. Elizabeth Rosado Balmayor, for her constant support, help, and guidance. I am deeply grateful for the opportunity to pursue my doctoral thesis in the Experimental Trauma Lab of the Technical University of Munich. Thank you to my mentor, Dr. Patrina Su Ping Poh, who guided and helped me anytime.

Thanks to the members of the Experimental Trauma Lab who supported me throughout the entire time of my experiments and the writing of my thesis. Thanks also to the members of the Musculoskeletal Gene Therapy Research Laboratory at Mayo Clinic (USA) for setting up the rat patellar enthesis model and performing the rat surgeries in previous studies.

I want to thank my friend, Alexandra von Stempel, for her considerate help.

The biggest thank you goes out to my family. My parents, Guenter and Katharina, who offered me the opportunity to study medicine and encouraged me on the way to achieve this. To my two siblings, Friederike and Julius, I am grateful for the consistent help and advice you have given me.

I would also like to say a special thank you to my uncle, Prof. Dr. med. Klaus Matzel, for his support and motivation during the entire time of my studies and my dissertation.